



הטכניון – מכון טכנולוגי לישראל
Technion – Israel Institute of Technology

ספריות הטכניון The Technion Libraries

בית הספר ללימודי מוסמכים ע"ש ארווין וג'ואן ג'ייקובס
Irwin and Joan Jacobs Graduate School



All rights reserved

*This work, in whole or in part, may not be copied (in any media), printed, translated, stored in a retrieval system, transmitted via the internet or other electronic means, except for "fair use" of brief quotations for academic instruction, criticism, or research purposes only.
Commercial use of this material is completely prohibited.*



כל הזכויות שמורות

אין להעתיק (במדיה כלשהי), להדפיס, לתרגם, לאחסן במאגר מידע, להפיץ באינטרנט, חיבור זה או כל חלק ממנו, למעט "שימוש הוגן" בקטעים קצרים מן החיבור למטרות לימוד, הוראה, ביקורת או מחקר. שימוש מסחרי בחומר הכלול בחיבור זה אסור בהחלט.

DIGITAL CYCLOTOMIC FILTERS AND THEIR
APPLICATIONS TO SIGNAL PROCESSING

PROJECT THESIS

Submitted in partial fulfillment of the requirements
for the degree of Master of Science
in Electrical Engineering

by

HERTZ DAVID

Submitted to the Senate of the Technion - Israel Institute of Technology

Sivan 5739

Haifa

June 1979



This final project was carried out
under the supervision of:
Dr. David Malach and
Professor Robert Kurshan
in the Signal Processing Laboratory,
Faculty of Electrical Engineering,
at the Technion -
Israel Institute of Technology, Haifa.

It is a great pleasure to thank
Dr. David Malach and
Professor Robert Kurshan,
for suggesting the subject,
their deep personal involvement
and for the help and patience they
have given me in all stages of this work.

Thanks are also due to the Laboratory Engineers
Yoram Or-Chen and Eli Polak,
for their sincere help
in carrying out the project.

To my father Shaul.,

CONTENTS

	<u>Page</u>
ABSTRACT	1
LIST OF SYMBOLS	3
Chapter 1: Introduction	9
Chapter 2: Properties of Cyclotomic Filters	11
2.1 Introduction	11
2.2 Description of Digital Cyclotomic Filters.	13
2.3 Properties of Cyclotomic Polynomials.	16
2.4 Properties of Digital Cyclotomic Filters.	21
2.4.1 Impulse Response	21
2.4.2 Resonant Frequencies	24
2.5 Eliminating In-Band Higher Order Resonances.	26
2.6 Computing word length and additions per cycle.	34
Chapter 3: Applications of Cyclotomic Filters	41
3.1 Introduction	41
3.2 FSK	41
3.3 A Touch-Tone [®] Receiver-Generator ²	41
3.4 Periodic Sequence Generators	44
3.5 A Bank of Single Tone Detectors	50
Chapter 4: The Cyclotomic Tone Detection System, Principle of Operation.	51
4.1 Introduction	51
4.2 Description of the Digital Filters in the CTD System	53

CONTENTS (Cont'd)

	<u>Page</u>
4.3 The Response of the Filters to a Sine Wave.	55
4.3.1 The Response of C_1 and C_2 to a Complex Input.	58
4.3.2 The Response of C_3 , C_6 to a Complex Input.	59
4.4 The Equivalent of Shifting the Input Frequency.	63
4.5 CTD System, Principle of Operation	64
Chapter 5: Detection Error Analysis of the CTD System	71
5.1 Introduction	71
5.2 Definitions of Probabilistic Quantities.	72
5.3 Error Analysis of a Pair of Cyclotomic Filters	73
5.3.1 The statistics of $n(t)$	75
5.3.2 The statistics of $n_R(t)$ and $n_I(t)$	77
5.3.3 The statistics of $z_R(N-1)$ and $z_I(N-1)$	81
5.4 Error Analysis at stage s_i .	91
5.4.1 Error Analysis at Stage I.	91
5.4.2 Error Analysis at Stages II, III	98
5.4.3 Error Analysis at Stage s using Repetitions.	98
Chapter 6: Computer Simulations of the CTD System	100
6.1 Introduction	100
6.2 The Simulation Program	101

CONTENTS (Cont'd)

	<u>Page</u>
6.2.1 Mathematical Concepts	101
6.2.2 The Description of the Simulation Program.	104
6.3 Description of the Model Program	105
6.4 Results	105
6.4.1 The CTD System without Repetitions	106
6.4.2 The Optimal CTD System	107
6.4.3 The Implemented CTD System	111
6.5 Comparison to a DFT Tone Detection System ⁽¹⁷⁾	113
Chapter 7: The Design and Construction of the CTD System.	121
7.1 Introduction	121
7.2 Specifications	122
7.3 CTD System Description	122
7.3.1 The Hilbert Network Unit.	124
7.3.2 The Digitizer Unit	124
7.3.3 The Parallel Buffer Unit	124
7.3.4 The Frequency Shifting Unit	125
7.3.5 The Cyclotomic Filters Unit	125
7.3.6 The Decision Unit	125
7.3.7 The Display Unit	125
7.3.8 The Main Control Unit	126
7.4 Description of the Hilbert Network Unit.	126
7.4.1 Design Considerations	126
7.4.2 The Hardware	126

CONTENTS (Cont'd)

	<u>Page</u>
7.5 Description of the Digitizer Unit Hardware	128
7.5.1 Design Considerations	128
7.5.2 The Digitizer Block Diagram	129
7.5.3 The Sample and Holds Modules	129
7.5.4 The Analog Multiplexer Module	130
7.5.5 The A/D Converter Module	130
7.5.6 The Digitizer Control	131
7.6 Description of the Parallel Buffer Hardware	132
7.6.1 Design Considerations	132
7.6.2 The Parallel Buffer Block Diagram	133
7.6.3 The Storage Module	135
7.6.4 The Selection Logic Hardware	136
7.6.5 The Read/Write Control Module	137
7.6.6 The Address Control Module	139
7.7 Description of the Frequency Shifting Unit Hardware	142
7.8 Description of the Filters Unit Hardware.	147
7.9 The Decision Unit Hardware	153
7.10 The Display Unit Hardware	155
7.11 The Main Control Unit Hardware	156
Chapter 8: Measurements	162
Chapter 9: Summary and Conclusions	164
Appendix A: Properties of Cyclotomic Polynomials	166
Appendix B: The Hilbert Network Design Program	182

CONTENTS (Cont'd)

	<u>Page</u>
Appendix C: The Simulation Program	187
Appendix D: The Model Program	197
Appendix E: An Analytic Expression to Calculate $(S/N)_o$	202
References	203

ABSTRACT

This thesis presents a new application of digital cyclotomic filters and its realization in hardware: "a bank of single tone detectors", named Cyclotomic Tone Detection (CTD) system.

Cyclotomic filters are all pole linear digital filters with their poles on the unit circle. Therefore, they can be used as receivers for single tone detection.

All cyclotomic filters have integer coefficients in the feedback loop and the coefficients of all the cyclotomic filters of interest are 0,1,-1. Therefore, cyclotomic filters operate without arithmetic roundoff error and all the cyclotomic filters of interest are implemented without multiplications - only additions and subtractions are needed

The CTD system is characterized by the property that the tone is detected with few simple cyclotomic filters and by properly changing the sampling rate in steps.

The input to the CTD system is a single tone with constant amplitude and frequency f that satisfies: $f \leq f_H$. The implemented CTD system detects in which of 64 ($=4^3$) cells of frequency bandwidth $f_H/64$ the tone is present. This task is performed in 3 stages. Each stage is characterized by a different sampling rate, the sampling rate at stage s is: $f_{c_s} = f_H/4^{s-2}$.

In the 1st stage ($f_{c_1} = 4f_H$) it is decided in which of 4 cells of frequency bandwidth $f_H/4$ the tone is present.

In the 2nd stage ($f_{c_2} = f_H$) the cell of frequency bandwidth $f_H/4$ detected in the 1st stage is divided by 4 and it is decided in which of the 4 cells of frequency bandwidth $f_H/16$ the tone is present.

In the 3rd stage ($f_{c_3} = f_H/4$) the cell of frequency bandwidth $f_H/16$ detected in the 2nd stage is divided by 4 and it is decided in which of 4 cells of frequency bandwidth $f_H/64$ the tone is present.

After completion of the 3rd stage the CTD system indicates in which of the 64 cells of frequency bandwidth $f_H/64$ the tone is present.

Generally one can have a CTD system with 4^L cells where L is the # of stages.

There are several parameters to be determined in the CTD system. The determination of these parameters by computer simulation results in the optimal CTD system. The optimal CTD system was not implemented due to hardware limitations. The implemented CTD system compromises performance with reduction in the amount of hardware.

The simulation program is capable of analysing a CTD system with given parameters. The input to the simulation program is a constant amplitude single tone with additive white Gaussian noise. Two performance measures are the output of the simulation program:

- a. $\tilde{P}_E(\beta)$: The fraction of trials which results in incorrect cell assignments as a function of the resolution β in cells unit.
- b. SNR_0 : The ratio of the variance of the frequency error before and after frequency estimation .

In the optimal CTD system \tilde{P}_E is minimized and SNR_0 is maximized for any given signal to noise ratio at the input: SNR_i .

In addition to the simulation program an analytic statistical model is derived. The output of the model program is the performance measure $P_E(\beta)$ and subsequently SNR_0 .

The results of the simulations, the model and the measurements were found to be in good agreement.

The advantage of the model is that for high signal to noise ratio at the input one needs an enormous amount of computer time to run the simulation program, while the computer time needed to run the model program is small , and is independent of SNR_i .

An exhaustive survey of cyclotomic filters, their characteristic cyclotomic polynomials and the applications of cyclotomic filters is also given in this thesis. The properties of cyclotomic filters and cyclotomic polynomials are given with full proofs. Known applications of cyclotomic filters are also briefly described. These are oscillators for tone generation, receivers for single tone detection and periodic sequence generation.

LIST OF SYMBOLS

A	: Tone's amplitude
a_i	: Coefficients of a cyclotomic filter
B	: Frequency bandwidth
b_i	: Fourier coefficient at the root i .
$C_m(z)$: Cyclotomic polynomial of order m
c_i	: Coefficients of the FIR filter
$C_m(j^k)$: Cyclotomic filter C_m with the input multiplied by j^k .
f	: Tone's frequency
f_0	: A desired frequency
f_H	: The highest tone's frequency
f_L	: The lowest tone's frequency
f_s	: The sampling rate
f_{cs}	: The clock rate at stage s .
\hat{f}	: Tone's estimated frequency.
h_n	: Impulse response
$\hat{h}(q)$: DFT of h_n
$H(z)$: z transform of h_n
$H(s)$: Transfer function of the analog LPF
$H_1(s), H_2(s)$: The transfer functions of the analog Hilbert network
$I_0(x)$: Modified Bessel function of order zero.
k	: 1. Memory of a cyclotomic filter 2. Number of instant.
L	: 1. Number of stages. 2. Transformation matrix: $x_{n+1} = Lx_n$

LIST OF SYMBOLS (Cont'd)

m	: Order of cyclotomic filter
M	1. Number of trials in the simulation program 2. $\sup x_n \quad n < N$
$m(\delta)$: A. threshold corresponding to a small frequency bandwidth δ , for a given cyclotomic filter.
N	: Number of samples a cyclotomic filter is operated
N_0	: Spectral density of white noise
N_s	: Number of repetitions at stage s
N_{12}	: Number of samples $C_1(C_2)$ is operated
N_{36}	: Number of samples $C_3(C_6)$ is operated
$n_0(t)$: White Gaussian noise at the input to the LPF
$n(t)$: Coloured Gaussian noise at the output of the LPF
$n_R(t)$: Coloured Gaussian noise at the real output of the Hilbert net.
$n_I(t)$: Coloured Gaussian noise at the imaginary output of the Hilbert network.
p	1. Period of the impulse response of C_p 2. The population proportion of failures
P	: Observed proportion of failures
p_1, p_2	: Lower and upper confidence limits in estimating p .
\bar{P}_D	: Average probability of detection for the CTD system
\bar{P}_E	: Average probability of detection error for the CTD system
\bar{P}_{e_s}	: Average probability of detection error at stage s for the CTD system.
p_i	: The i^{th} prime in the prime decomposition of m .

LIST OF SYMBOLS (Cont'd)

- $Pe_s(\theta_s)$: Probability of detection error at stage s
as a function of $\theta_s = 2\pi f/f_{c_s}$
- $Pe_s(\theta_s)|C_1$: $Pe_s(\theta_s)$ constrained to C_1
- $Pe_s(\theta_s)|C_6, C_3(j^k)$: $Pe_s(\theta_s)$ constrained to the comparison
between C_6 and $C_3(j^k)$
- $R_{n_0}(\tau), R_n(\tau), R_{n_I}(\tau), R_{n_R}(\tau)$: The autocorrelation of $n_0(t),$
 $n(t), n_I(t), n_R(t)$
- $R(N)$: Maximum number of repetitions at each stage as a
function of N , for 256 data words.
- $R_{n_I n_R}(\tau)$: Cross correlation of $n_I(t)$ and $n_R(t)$
- $S_{n_0}(\omega), S_n(\omega), S_{n_R}(\omega), S_{n_I}(\omega)$: Spectral density of $n_0(t),$
 $n(t), n_R(t), n_I(t)$
- $S_{n_I n_R}(\omega)$: Cross spectral density of $n_I(t)$ and $n_R(t)$
- SNR_i : Signal to noise ratio at the input in db.
- $(S/N)_0$: proportion of frequency variance before and after
frequency estimation
- SNR_0 : $(S/N)_0$ in db
- TR1 : Threshold attached to $C_1(C_2)$ in the CTD system
- TR6 : Threshold attached to $C_3(C_6)$ in the CTD system.
- t : Time
- $U(z)$: z transform of u_n
- $u(t)$: Unknown tone
- u_n : Unknown tone; $A \sin(2\pi f n \tau + \phi)$ at instant n .

LIST OF SYMBOLS (Cont'd)

- $u_R(k)$: Tone's real component at instant k
- $u_I(k)$: Tone's imaginary component at instant k
- $\underline{u}(k)$: Complex tone at instant k ; $u_R(k)+ju_I(k)$
- v_n : Output of FIR filter preprocessing the input to a cyclotomic filter
- $v_R(k)$: Tone's real component without noise at instant k .
- $v_I(k)$:Tone's imaginary component without noise at instant k
- $\underline{v}(k)$: Complex tone without noise $v_R(k)+jv_I(k)$
- $W(z)$: z transform of c_n (FIR filter)
- $W^I(z)$: $W(z)$ with the coefficients rounded to the nearest integer
- w : Word length
- $X(z)$: z Transform of x_n
- \bar{x}_n : A vector $(x_n, x_{n-1}, \dots, x_{n-k+1})$
- $x_R(N-1)$: Clean real component of the output of C after N samples
- $x_I(N-1)$: Clean imaginary component of the output of C after N samples
- $\underline{x}(N-1)$: Clean complex output of C_m ; $x_R(N-1)+jx_I(N-1)$
- y_n : Output of a FIR filter at instant n attached to the output of a cyclotomic filter C .
- $z_C(n,\theta)$: Output of cyclotomic filter C at instant n due to a tone with normalized frequency θ
- $z_R(N-1)$: Real component of the output of a cyclotomic filter at instant $N-1$ (N samples)
- $z_I(N-1)$: Imaginary component of the output of a cyclotomic filter at instant $N-1$ (N samples)

LIST OF SYMBOLS (Cont'd)

- $\underline{z}(N-1)$: Complex output of a cyclotomic filter at instant
 $N-1$: $z_R(N-1) + jz_I(N-1)$ (N samples)
- z_c : Number of standard units corresponding to a given
confidence level.
- ϕ, ϕ_1, ψ : Phase angles in radians
- τ : 1. Time period of a clock
2. Time delay
- δ : A small frequency interval around f_0 .
- $\psi(m)$: The Euler ψ -function which gives the degree of the
polynomial $C_m(z)$.
- ρ_i : The i^{th} primitive m^{th} root of unity of $C_m(z)$.
- ρ_1 : The fundamental primitive m^{th} root of unity of $C_m(z)$
- α_i : The power of p_i in the prime decomposition of m
- $\mu(n)$: The Moebius function (2.10), n is an integer.
- $\mu(z)$: The unit step function
- $\theta(\ell)$: The angle of ρ_ℓ
- $\delta(\tau)$: The Dirac delta function
- α : A variable; 1 or j
- σ_{in}^2 : The power of $n(t)$
- β : Resolution in cells unit
- σ_{out}^2 : Power of noise at the output of the cyclotomic filter C_j
after N samples.
- ω : Angular frequency
- ω_0 : A desired angular frequency

List of Abbreviations

CTD: Cyclotomic tone detection

DFT: Discrete Fourier transform

C_m : Cyclotomic filter of order m .

CHAPTER 1

INTRODUCTION

This thesis presents a new application of digital cyclotomic filters: "a bank of single tone detectors", named - Cyclotomic Tone Detection (CTD) System.

The CTD system is realized in hardware. The CTD system is based on digital cyclotomic filters. Cyclotomic filters are all pole linear digital filters with poles on the unit circle. They have integer coefficients in the feedback loop and operate without arithmetic roundoff.

All the filters of interest have coefficients 0, ± 1 , hence multiplications are not needed and the filters are simple to implement.

The thesis is organized as follows:

In Chapter 2 cyclotomic filters are presented. Properties of cyclotomic polynomials are listed, with the detailed proofs given in appendix A. Properties of cyclotomic filters are given such as impulse response and resonant harmonics.

Methods of eliminating in-band higher order resonances are presented. These methods are transversal FIR filters at the input or at the output. Methods for implementing the transversal filters are described. Word length and additions per cycle are computed for various cyclotomic filters.

Chapter 3 describes the applications of cyclotomic filters. Cyclotomic filters have their poles on the unit circle, therefore they may be used as generators and as receivers for a single tone. Various applications were suggested by R. Kurshan and B. Gupinath^(1,2,3,4). These applications are: FSK generation and detection, a Touch-Tone[®] Receiver-Generator and periodic sequence generation.

A new application of cyclotomic filters: "a bank of single tone detectors" is proposed in this work and the description of its hardware realization is given.

The new application is described in detail in Chapters 4 to 7.

Chapter 4 describes the principle of operation of the proposed Cyclotomic Tone Detection (CTD) System. The CTD system is based on cyclotomic filters of the 1st and 2nd degree. With few simple filters and by changing the clock rate in steps the tone is detected.

Chapter 5 gives the error analysis of the CTD system. A model that describes the performance of the CTD system in the presence of a noisy tone is proposed.

Chapter 6 describes the simulation program and the model program. Results of the simulation and model are in good agreement. CTD system parameters for optimal performance are found from the simulations and the model.

The implemented CTD system is a compromise. The performance of the implemented CTD system is found from the simulation and the model programs. The performance of the CTD system is also compared to the performance of a DFT tone detection system.

Chapter 7 describes the design and construction of the CTD system.

Chapter 8 gives the results of the measurements from the implemented CTD system and a comparison to the simulation results. The results of the measurements and simulations are in good agreement.

Chapter 9 gives a summary and draws conclusions. A new way to realize cyclotomic filters is proposed.

CHAPTER 2

PROPERTIES OF CYCLOTOMIC FILTERS

2.1 Introduction

Cyclotomic filters are a class of digital filters that operate without arithmetic roundoff. These filters are all pole linear digital filters, and can be used both as oscillators for tone generation and also as receivers for single tone detection.

Generally, tones for signaling are analog signals of the form $A \sin(\omega t + \phi)$. (A is the amplitude, $2\pi/\omega$ is the period and ϕ is the phase).

The feedback loop of each filter is constructed in such a way as to eliminate the possibility of roundoff or truncation errors, thus insuring perfect arithmetic. This entirely eliminates the problem of limit cycles. The presented filters, when used as generators, produce quantized values of $A \sin \omega t$ of arbitrary amplitude accuracy ⁽¹⁾.

Implementation of these filters as receivers involves first sampling an analog input signal to produce a digital input into the filter. The filter is designed to resonate for a particular frequency. Thus enabling detection.

The means by which arithmetic errors are eliminated in the feedback loop is by constraining all feedback coefficients to be integers, a constraint necessary to guarantee perfect arithmetic in any digital filter. Thus multiplication by these coefficients can be performed as additions, simplifying implementation.

The behavior of the feedback loop of this filter is modeled by a linear recursion whose characteristic polynomial is a cyclotomic polynomial. In recognition of this, we call the filter consisting of the feedback loop alone a "cyclotomic filter". In ⁽¹⁾ it is shown that the only way to ensure perfect arithmetic and thus avoid limit cycles in a digital filter is to constrain the feedback coefficients to be integers. Furthermore, it is shown in ⁽¹⁾ with this constraint on the coefficients and also subject to minimizing memory and eliminating as many resonant harmonics as possible, the cyclotomic filter is uniquely optimal among all digital linear filters, both for the purpose of tone generation and tone detection.

Applications of cyclotomic filters are tone generators of arbitrary amplitude accuracy and tone detectors ⁽¹⁾. Devices for tone generation and detection have widespread applications. The most notable examples are Touch-Tone[®] signaling ⁽²⁾, and frequency shift keying (FSK) ⁽¹⁾. Periodic sequence generation is another application ^(3,4).

Section 2.2 gives a description of digital cyclotomic filters.

Section 2.3 summarizes the properties of Cyclotomic Polynomials ^(5,6,7,8,10).

Section 2.4 gives the properties of digital cyclotomic filters ^(1,5).

Section 2.5 explains how to eliminate in band higher order resonances using a transversal filter.

Section 2.6 explains how to compute word length and additions per cycle, i.e., period of cyclotomic filter.

2.2 Description of Digital Cyclotomic Filters

Cyclotomic filters are a special class of recursive filters of the form:

$$x_n = \sum_{i=1}^k a_i x_{n-i} + u_n \quad (2.1)$$

The numbers a_i ($i=1, \dots, k$) are the feedback coefficients of the filter. The filter is driven by a clock with time interval τ between pulses. In tone generation the filter must satisfy.

$$x_n = u(n\tau) \quad (2.2)$$

at least for some initial conditions x_0, \dots, x_{k-1} . When used as a receiver the analog input $u(t)$ is sampled producing a discrete input $u_n = A \sin(\omega_0 n\tau + \phi)$

The filter (2.1) must distinguish between the desired frequency f_0 and all other frequencies in a band containing f_0 .

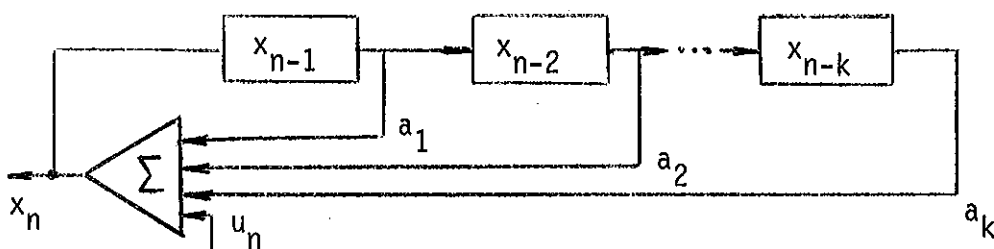


Fig. 2.1: Recursive filter in k stages of memory.

ציור 2.1: מסנן רקורסיבי בעל k שלבי זכרון.

Specifically, it must satisfy the resonance property.

$$\limsup_{n \rightarrow \infty} |x_n| = \infty \quad (2.3)$$

$n \rightarrow \infty$

When $f = f_0$, and in a sufficiently large band B including f_0 there must be no other such resonances. Then $|x_n|$ will be uniformly bounded in B in the complement of any small interval δ about f_0 , say, $|x_n| < m(\delta)$ for all $f \in B$, $f \notin \delta$, for all n . A threshold detector can thus, detect in a finite amount of time N , the presence (or absence) within B of an input frequency f_0 (with error $\pm \frac{1}{2} |\delta|$). It does this by comparing the gain $\sup_{n < N} |x_n|$ with the bound $m(\delta)$. If $\sup_{n < N} |x_n| < m(\delta)$, then $f \in \delta$ otherwise it is not.

Of course the smaller the allowable error δ , the larger N must be.

Fig. 2.2 is a tone detector suggested in ⁽¹⁾ based on the previous ideas.

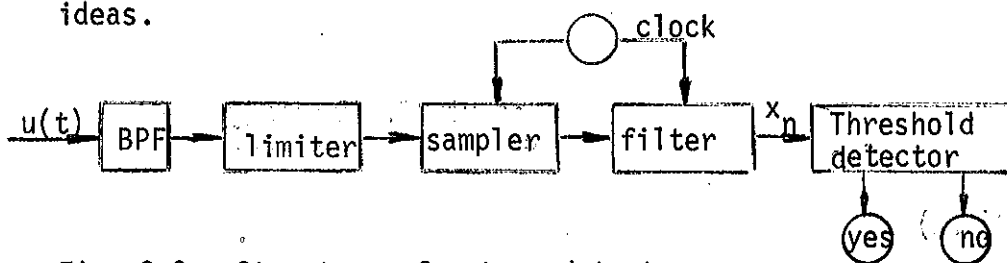


Fig. 2.2: Structure of a tone detector.

ציוור 2.2: מבנה של גלאי טונים

The z transform of 2.1 gives:

$$\frac{X(z)}{U(z)} = \frac{1}{1 - \sum_{i=1}^k a_i z^{-i}} \quad (2.4)$$

The characteristic equation is:

$$z^k - \sum_{i=1}^k a_i z^{k-i} \approx 0 \quad (2.5)$$

and $\rho_1, \rho_2, \dots, \rho_k$ are the roots of (2.5).

In the case of cyclotomic filters (2.5) is a cyclotomic polynomial.

Example 2.1: Cyclotomic polynomial of order 9 - $C_9(z)$

Suppose we want to find the cyclotomic polynomial of order 9, then:

$$\rho_1 = e^{j 2\pi/9} ; \quad j = \sqrt{-1}$$

The other roots are $(\rho_1)^\ell$, $1 < \ell < 9$ where ℓ has no common factor with 9, briefly $(\ell, 9) = 1$ (the g.c.d. of ℓ and 9 is 1). Hence the roots are:

$$\rho_1, \rho_1^2, \rho_1^4, \rho_1^5, \rho_1^7, \rho_1^8$$

and the cyclotomic polynomial is:

$$C_9(z) = \prod_{\substack{\ell=1 \\ (\ell, 9)=1}}^9 (z - \rho_1^\ell) = z^6 + z^3 + 1$$

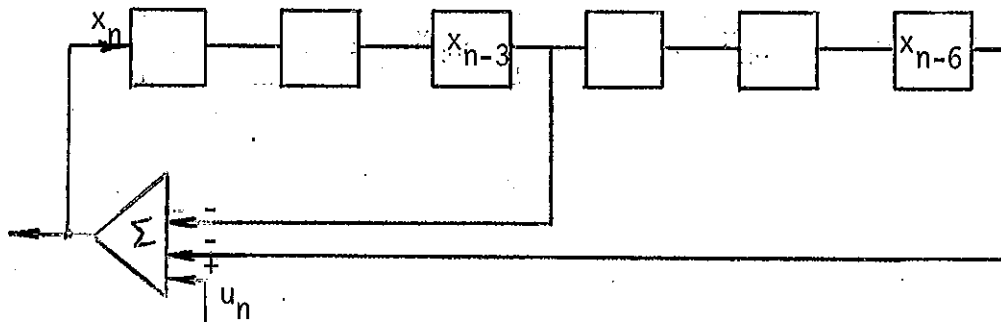


Fig. 2.3: Cyclotomic filter C_9 in 6 stages of memory.

ציור 2.3: מסנן ציקלוטומי C_9 בעל 6 דרגות זכרון.

Note that the memory k is equal to the degree of the cyclotomic polynomial, which is determined by the order of the cyclotomic filter. (the order of the cyclotomic polynomial is greater than its degree).

2.3 Properties of Cyclotomic Polynomials

A summary of the properties of cyclotomic polynomials is given in this section. For a detailed presentation refer to appendix A. Cyclotomic filters are a class of digital filters. Therefore, we shall confine ourselves to cyclotomic polynomials whose roots are in the Complex field. The roots of the cyclotomic polynomial $C_n(x)$ are all the distinct primitive n^{th} roots of unity, hereforth defined.

Definition 2.1

ρ is a primitive n^{th} root of unity if $\rho^n = 1$ and $\rho^m \neq 1$ for $0 < m < n$. We also say that the order of ρ is n .

$\rho = e^{j 2\pi/n}$ is the fundamental primitive n^{th} root of unity.

If ρ is a primitive n^{th} root of unity, every other primitive n^{th} root of unity is of the form ρ^m where $(n,m)=1$ (the g.c.d. of m and n is 1). There are as many distinct primitive n^{th} roots of unity as there are positive integers less than n , which have no common factor with n .

Next cyclotomic polynomials are defined and an example is given.

Definition 2.2

A cyclotomic polynomial of order n denoted $C_n(x)$ is the polynomial whose roots are all the primitive n^{th} roots of unity.

$$C_n(x) = \prod_{i=1}^{\psi(n)} (x - \rho_i) \quad (2.6)$$

where $\rho_1, \rho_2, \dots, \rho_{\psi(n)}$ are the distinct primitive n^{th} roots of unity, and $\psi(n)$ is their number. $\psi(n)$ is the Euler ψ -function.

Notes:

- a) the degree of C_n is $\psi(n) \leq n$
- b) each ρ_i can be expressed as $\rho_i = \rho^{m_i}$ for some primitive n^{th} root of unity ρ and positive integers $m_i < n$.

Example 2.2:

For $C_6(x)$ $\rho_1 = e^{j 2\pi/6}$, $\rho_2 = e^{j(2\pi/6)5}$

$$C_6(x) = (x - \rho_1)(x - \rho_2) = x^2 - x + 2 \text{ and } \psi(6) = 2$$

If $n = \prod p_i^{\alpha_i}$ (prime decomposition) then $\psi(n) = \prod p_i^{\alpha_i - 1} (p_i - 1)$

e.g. $n = 180 = 2^2 \cdot 3^2 \cdot 5$ then -

$$\psi(180) = 2^{2-1} (2-1) \cdot 3^{2-1} (3-1) \cdot 5^{1-1} \cdot (5-1) = 48$$

The following are properties of cyclotomic polynomials:

$$x^n - 1 = \prod_{\substack{d|n}} C_d(x) \quad (2.7)$$

From (2.7) one can conclude that

$$n = \sum_{\substack{d|n}} \psi(d) \quad (2.8)$$

$$C_n(x) = \prod_{d|n} (x^d - 1)^{\mu(n/d)} = \prod_{d|n} (x^{n/d} - 1)^{\mu(d)} \quad (2.9)$$

where $\mu(d)$ is the Moebius function defined by:

$$\mu(d) = \begin{cases} 1 & \text{if } d=1 \\ (-1)^k & \text{if } d \text{ is a product of } k \text{ distinct primes} \\ 0 & \text{if } d \text{ contains any repeated prime factors} \end{cases} \quad (2.10)$$

Example 2.3:

$$C_{105}(x) = ?$$

$105 = 3 \cdot 5 \cdot 7$ hence by (2.9).

$$C_{105}(x) = \frac{(1-x^3)(1-x^5)(1-x^7)(1-x^{105})}{(1-x)(1-x^{15})(1-x^{21})(1-x^{35})}$$

If p is a prime, then:

$$C_p(x) = x^{p-1} + x^{p-2} + \dots + 1 \quad (2.11)$$

and for any power of p

$$C_{p^m}(x) = C_p(x^{p^{m-1}}) \quad (2.12)$$

$$C_{mp^k}(x) = C_{mp}(x^{p^{k-1}}) \quad (2.13)$$

A conclusion from 2.13 is that:

$$C_{p_1^{\alpha_1} \dots p_\ell^{\alpha_\ell}}(x) = C_{p_1 p_2 \dots p_\ell} \left(x^{p_1^{\alpha_1-1} \dots p_\ell^{\alpha_\ell-1}} \right) \quad (2.14)$$

(p_i distinct primes).

From (2.14) follows that most of the coefficients of C_m for m highly factorable will usually be zeroes, and hence the number of taps - to - memory ratio is generally low.

In practice (2.14) prove quite helpful in simplifying calculations. Using (2.14), the calculation may be reduced to a case where n is the product of distinct primes.

→ If p is a prime and $p \nmid m$, then

$$C_{pm} = \frac{C_m(x^p)}{C_m(x)} \quad (2.15)$$

→ If $n \geq 3$ and n odd - then

$$C_{2n}(x) = C_n(-x) \quad (2.16)$$

$$C_n(1) = \begin{cases} 0 & \text{iff } n=1 \\ p & \text{iff } n \text{ is a power of the prime } p \\ 1 & \text{iff } n \text{ has two or more distinct prime factors.} \end{cases} \quad (2.17)$$

$$C_n(-1) = \begin{cases} 0 & \text{iff } n=2 \\ -2 & \text{iff } n=1 \\ 2 & \text{iff } n \text{ is a power of } 2, n \geq 4 \\ p & \text{iff } n \text{ is } 2 \text{ times a power of } p \\ 1 & \text{otherwise} \end{cases} \quad (2.18)$$

In practice (2.17) and (2.18) provide helpful checks on the result.

$$\text{If } n \geq 2 \text{ and } C_n(x) = \sum_{i=0}^{\psi(n)} a_i x^i, \text{ then for all } i:$$

$$a_i = a_{\psi(n)-i} \quad (2.19)$$

So, to compute $a_0, \dots, a_{\psi(n)}$, it is sufficient to compute only the first $\psi(n)/2+1$ coefficients ($\psi(n)$ is even except for C_1 and C_2)

Example 2.4:

Let us determine $C_{36}(x)$ by (2.14)

$$C_{36}(x) = C_{2^2 \cdot 3^2}(x) = C_{2 \cdot 3}(x^{2 \cdot 3}) = C_6(x^6)$$

By example 2.2:

$$C_6(x) = x^2 - x + 1 \text{ hence,}$$

$$C_{36}(x) = x^{12} - x^6 + 1.$$

- For all n , $C_n(x)$ has integer coefficients.

- $C_n(x)$ is irreducible over Q (the rational field).
- If $f(x)$ is a monic polynomial with integer coefficients and every root r of $f(x)$ satisfies $|r| \leq 1$, then $f(x) = x^m \prod_n C_n(x)$.
- Cyclotomic polynomials make very desirable characteristic polynomials because of their extremely simple structure. For example, for $m < 105$ or for m a product of two primes the coefficients of $C_m(x)$ are all 0, ± 1 . For m a power of a single prime, the coefficients are all 0, 1. For $m < 385$ the coefficients do not exceed 2 in absolute value. If m is a product of 3 distinct primes, all the coefficients are less than the smallest of those primes. As n runs over all products of three distinct primes, the cyclotomic polynomials $C_n(x)$ contain arbitrarily large coefficients. Those assertions are cited in (6).

2.4 Properties of Digital Cyclotomic Filters

2.4.1 Impulse response

The impulse response is the output resulting from an input of a single pulse: $u_0=1, u_n=0, |n| > 0$. It is shown in the sequel that the impulse response of the cyclotomic filter C_m is periodic of period m , therefore we will refer to h_n as a pulse train. From difference equations theory it follows that the impulse response h_n of the cyclotomic filter C_m having $\psi(m)$ poles is given by

$$h_n = \sum_{i=1}^{\psi(m)} b_i p_i^n \quad (2.20)$$

Since each ρ_i is a primitive m^{th} root of unity, the sequence h_n is periodic:

$$h_{n+m} = h_n \text{ for all } n.$$

The proof is simple:

$$h_{n+m} = \sum b_i \rho_i^{n+m} = \sum b_i \rho_i^n \rho_i^m = \sum b_i \rho_i^n = h_n$$

Let $\hat{h}(q)$ be the DFT of h_n then:

$$\hat{h}(q) = \frac{1}{m} \sum_{n=0}^{m-1} h_n e^{-j2\pi(q/m)n} \quad (2.21)$$

Then:

$$\hat{h}(q) = \frac{1}{m} \sum_{n=0}^{m-1} \left(\sum_{i=1}^k b_i \rho_i^n \right) e^{-j2\pi(q/m)n} = \frac{1}{m} \sum_{i=1}^k b_i \sum_{n=0}^{m-1} \rho_i^n e^{-j2\pi(q/m)n} =$$

$$\hat{h}(q) = \begin{cases} b_\ell & \text{if there exists a root } \rho_\ell \text{ such that } \rho_\ell = e^{j(2\pi/m)q} \\ 0 & \text{if no such root } \rho_\ell \text{ exists.} \end{cases} \quad (2.22)$$

To simplify matters we shall use the expression "The Fourier coefficient at (the root) ρ_ℓ " to indicate what, in the case of (2.22) is the q^{th} Fourier coefficient $\hat{h}(q)$.

It will be shown that the b_ℓ 's are given by:

$$b_\ell = \prod_{\substack{i=1 \\ i \neq \ell}}^k \frac{\rho_\ell}{\rho_\ell - \rho_i} \quad (2.23)$$

By (2.4) the z transform of h_n is

$$H(z) = \frac{1}{1 - \sum_{i=1}^k a_i z^{-i}} = \prod_{i=1}^k \frac{1}{(1 - \rho_i z^{-1})} \quad (2.24)$$

Taking the z transform of (2.20) gives:

$$H(z) = \sum_{i=1}^k b_i \frac{1}{1 - \rho_i z^{-1}} \quad (2.25)$$

then:

$$b_\ell = \lim_{z^{-1} \rightarrow \rho_\ell} \left[\prod_{i=1}^k \frac{1}{1 - \rho_i z^{-1}} \cdot (1 - \rho_\ell z^{-1}) \right] = \prod_{\substack{i=1 \\ i \neq \ell}}^k \frac{\rho_\ell}{\rho_\ell - \rho_i}$$

Substituting $\lambda = z^{-1}$ gives:

$$H(\lambda) = \frac{1}{C_m(\lambda)} \quad (2.26)$$

$$\text{But } H(\lambda) = \sum_{n=0}^{\infty} h_n \lambda^n = \left(\sum_{n=0}^{m-1} h_n \lambda^n \right) \left(\sum_{k=0}^{\infty} \lambda^{mk} \right)$$

since $h_{n+m} = h_n$. Defining $f(\lambda) = \sum_{n=0}^{m-1} h_n \lambda^n$, one obtains:

$$f(\lambda) = \frac{1 - \lambda^m}{C_m(\lambda)} \quad (2.27)$$

Notice that f has integer coefficients (the input δ_n is integer, as are the coefficients a_i).

Indeed $1-\lambda^m$ is a product of cyclotomic polynomials one of which is $C_m(\lambda)$. Specifically:

$$1-\lambda^m = - \prod_{n|m} C_n(\lambda)$$

and from (2.26)

$$f(\lambda) = - \prod_{\substack{n|m \\ n \neq m}} C_n(\lambda) \quad (2.28)$$

Consequently, $f(\rho) = 0$ for all n^{th} roots of unity, except for the primitive roots of unity

2.4.2 Resonant Frequencies

Let $u_n = e^{j(2\pi f n \tau + \phi)}$ then

$$x_n = \sum_{i=0}^n h_{n-i} x_i \quad \text{where}$$

$$h_n = \sum_{\ell=1}^{\psi(m)} b_{\ell} \rho_{\ell}^n \quad \text{and} \quad \rho_{\ell} \triangleq e^{j\theta(\ell)} \quad \text{then}$$

$$x_n = \sum_{i=0}^n \left(\sum_{\ell=1}^{\psi(m)} b_{\ell} \rho_{\ell}^{n-i} \right) u_i = \sum_{\ell=1}^{\psi(m)} b_{\ell} \sum_{i=0}^n \rho_{\ell}^{n-i} e^{j(2\pi f \tau i + \phi)}$$

$$= \sum_{\ell=1}^{\psi(m)} b_{\ell} \sum_{i=0}^n e^{j\theta(\ell)} (n-i) e^{j(2\pi f \tau i + \phi)}$$

$$= e^{j\phi} \sum_{\ell=1}^{\psi(m)} b_{\ell} \frac{1 - e^{j[2\pi f \tau - \theta(\ell)]} (n+1)}{1 - e^{j[2\pi f \tau - \theta(\ell)]}} \quad (2.29)$$

The resonance condition is:

$$2\pi f\tau - \theta(q) = 2\pi r$$

$$r = 0, \pm 1, \pm 2, \dots \quad (2.30)$$

Since if (2.30) is satisfied for some q the sum (2.29) contains a summand $e^{j\phi} \cdot b_q(n+1)$ that tends to infinity as n tends to infinity.

As the roots are all of the form: $\exp [2\pi j(d/m)]$, the resonant frequencies can be expressed as:

$$2\pi f\tau = 2\pi \frac{d}{m} \pmod{2\pi} \quad (2.31)$$

for all positive integers $d < m$ such that $(d, m) = 1$. Resonance at the fundamental is described by $2\pi f\tau = 2\pi(1/m)$, that is the fundamental of the filter is $f = \tau^{-1}/m$. Hence, if one requires a fundamental frequency of f_0 (i.e., if f_0 is the frequency of the tone to be generated or detected) and one intends to use a filter with memory $k = \psi(m)$, the clock rate τ^{-1} is set at $\tau^{-1} = f_0 m$. All other resonances occur at various harmonics (multiples of f_0) as follows:

The resonant harmonics in the band $0 \leq f \leq \tau^{-1}$ occur when $f\tau = d/m$ that is, at $f = df_0$ for all those integers d as above. For example, if $m = 30$, then $\psi(30) = 8$ and d assumes the values 1, 7, 11, 13, 17, 19, 23, 29. Hence, this filter has no resonances between the fundamental f_0 and the seventh harmonic. It resonates at the seventh harmonic $7f_0$, and thereafter at $11f_0$, $13f_0$, and so on.

The first resonance due to aliasing will always be at $f = f_0 + \tau^{-1} = f_0 + f_0 m = f_0(m+1)$. In the case of the previous example, this is the thirty-first harmonic.

2.5 Eliminating in-band higher order resonances⁽¹⁾

The preceding analysis has indicated that, within the constraints established, various higher-order resonances are unavoidable. This could lead to difficulties. In practice, many higher-order harmonics are introduced in the process of limiting the input signal. The limiter (see Fig. 2.2) limits the amplitude of the input signal $u(t)$. For example, a common limiter is a "hard-clipper". This has output ± 1 , depending on whether $u(t) \geq 0$, or $u(t) < 0$. The effect of hard clipping of the input signal is to produce all the odd harmonics: $\sin 2\pi f\tau \rightarrow 2/\pi \sin 2\pi f\tau + 2/3\pi \sin 6\pi f\tau + 2/5\pi \sin 10\pi f\tau + \dots$. Hence, a filter with more resonances must be run for a longer period of time to attain a threshold sufficiently high to reject spurious signals. Also, when used as a generator, perturbations of the initial conditions of the filter could lead to unwanted harmonics at all the resonances of the filter. As such perturbations are inevitable, it is usually necessary to make allowance for eliminating these harmonics.

While resonances due to aliasing are inherent to the discrete-time nature of the system and are hence unavoidable, resonances below the clock frequency τ^{-1} can be handled outside the feedback loop. This is accomplished either through alteration of the input before it enters the filter: $u_n \rightarrow v_n = \sum_{i=0}^d c_i u_{n-i}$ or equivalently through alteration of the filter output before it enters the threshold detector: $x_n \rightarrow y_n = \sum_{i=0}^d c_i x_{n-i}$. (see Fig. 2.4a and Fig. 2.4b respectively). Although these two options are mathematically equivalent, considerations with respect to minimizing the word length necessary for perfect arithmetic would point in favor of one or the other. This will be discussed in section 2.6.

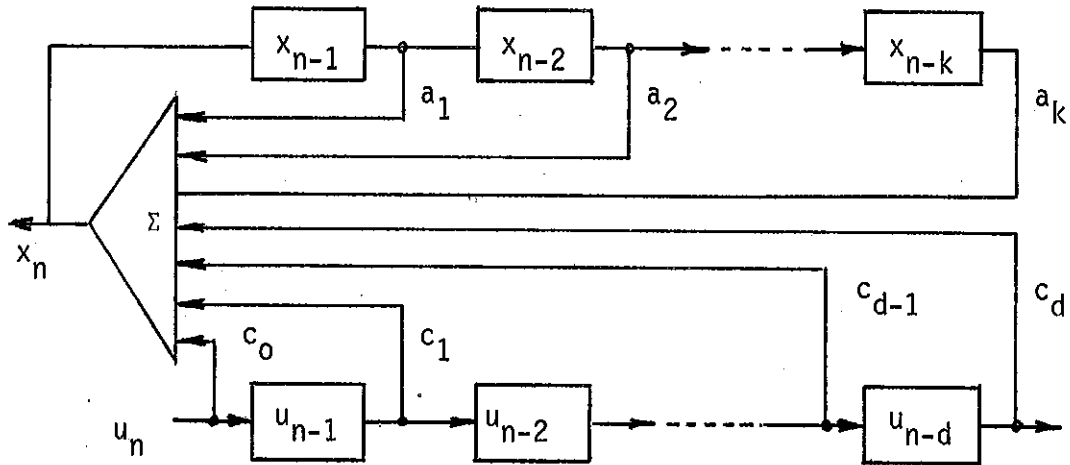


Fig. 2.4a: Implementation of the weighting function at the input.

ציור 2.4a: מימוש פונקציית המשקל בכניסה.

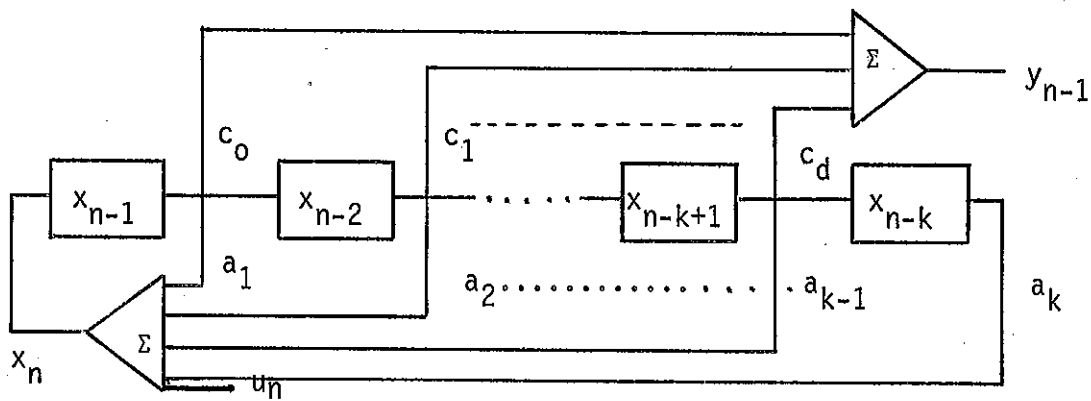


Fig. 2.4b: Implementation of the weighting function at the output.

ציור 2.4b: מימוש פונקציית המשקל ביציאה.

The weighting function $W(z)$ is a FIR filter. For Fig. 2.4a we have:

$$X(z) = \left[\frac{U(z)}{C_m(z^{-1})} \right] W(z) \quad (2.32a)$$

For fig. 2.4(b) we have

$$Y(z) = [W(z)U(z)] \frac{1}{C_m(z^{-1})} \quad (2.32b)$$

$W(z)$ has the property that $W(z)/C_m(z^{-1})$ has poles only at those roots of $C_m(z)$ corresponding to those resonances actually desired. Specifically $W(z)$ will be a polynomial of z^{-1} of degree $k-2r$ where r is the number of resonances desired in the band $[0, (2\tau)^{-1}]$. The zeroes of $W(z)$ will be those roots of $C_m(z)$ corresponding to the unwanted resonances. Typically, one desires to eliminate all resonances but the fundamental, in which case $r=1$ and

$$\frac{Y(z)}{U(z)} = \frac{W(z)}{C_m(z^{-1})} = \frac{1}{z^{-2} - az^{-1} + 1} \quad (2.33)$$

for Fig. 2.4a, 2.4b one obtains:

$$x_n = ax_{n-1} - x_{n-2} + u_n \quad (2.34a)$$

$$y_n = ay_{n-1} - y_{n-2} + u_n \quad (2.34b)$$

If ρ is the fundamental primitive m^{th} root of unity then:

$$(z^{-1} - \rho)(z^{-1} - \bar{\rho}) = z^{-2} - az^{-1} + 1$$

hence:

$$a = 2\text{Re}(\rho) \quad (2.35)$$

Although there will be truncation errors in (2.34), this will not lead to limit cycles, as there is no feedback from this to the filter. The arithmetic of the weighing function is only

approximate; since there is truncation error in the computation of the coefficients c_j . The zeroes of $W(z)$ will not precisely cancel out the roots of $C_m(z)$. Rather the roots of W will be slightly perturbed from the corresponding roots of $C_m(z)$. The effect of this, as will be shown is that all the resonances due to the roots of $C_m(z)$ will be present in the output however they will have reduced energy (but for the fundamental). That is, the less the error in the implementation of W , the smaller the Fourier coefficients of the higher order resonant harmonics of the filter. From the properties of DFT the Fourier coefficient of the output with a weighing function at the root ρ_j is $W(\rho_j)b_j$. The conjugate coefficient $W(\bar{\rho}_j) = \overline{W(\rho_j)}$, observe that, if ρ_j is a root of W then the Fourier coefficient of y_n vanishes at the roots ρ_j and $\bar{\rho}_j$. (W was chosen to be real).

If W' is the result of perturbing the coefficients of W to correspond to truncation error, then $W'(\rho_j)$ is (by continuity) close to zero. Hence, as errors in the weighing functions are reduced, so is the power at each of the resonant harmonics above the fundamental (running the system for finite time, of course).

If the coefficients of W' are simply those of W rounded to the nearest integer, the results are frequently virtually as good as if W itself were used. This is exhibited in Table 2.1 and illustrated in Figs. 2.5, 2.6, 2.7. These figures correspond to a filter using the cyclotomic polynomial C_{30} . The input is a hard clipped sine wave for each given frequency up to 15 times the fundamental frequency.

For each input frequency, the filter C_{30} is run for an amount of time which equals to 7 cycles of the fundamental $N = 7 \cdot 30 = 210$. The output is $\max_{n < N} |X_n|$ as measured at each input frequency (1500 samples).

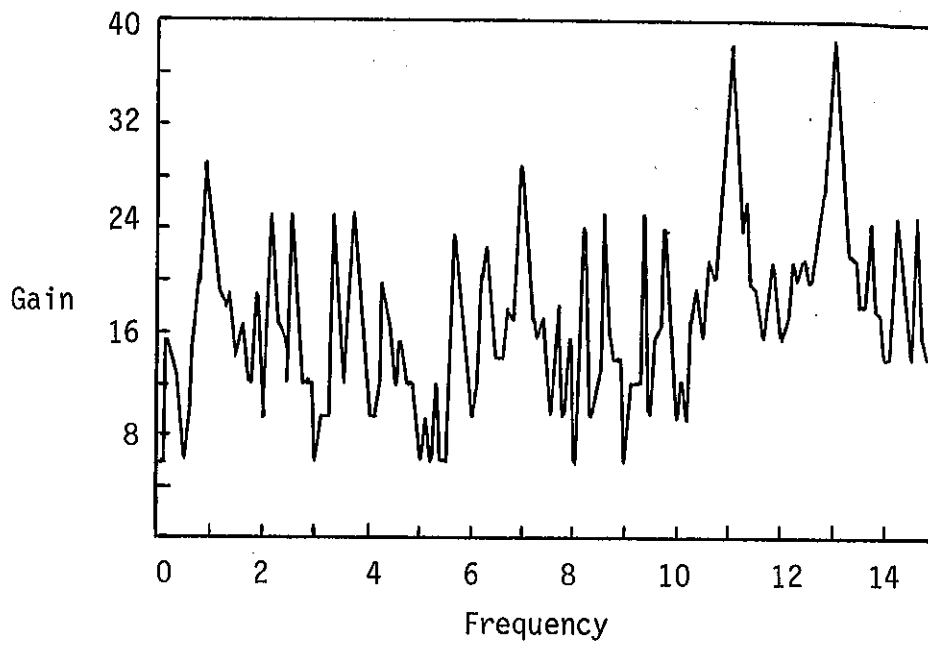


Fig. 2.5: Hard clipped, no weighting, C_{30} , 7 cycles.⁽¹⁾

ציור 2.5: hard clipped, ללא FIR, C_{30} , 7 מחזורים⁽¹⁾

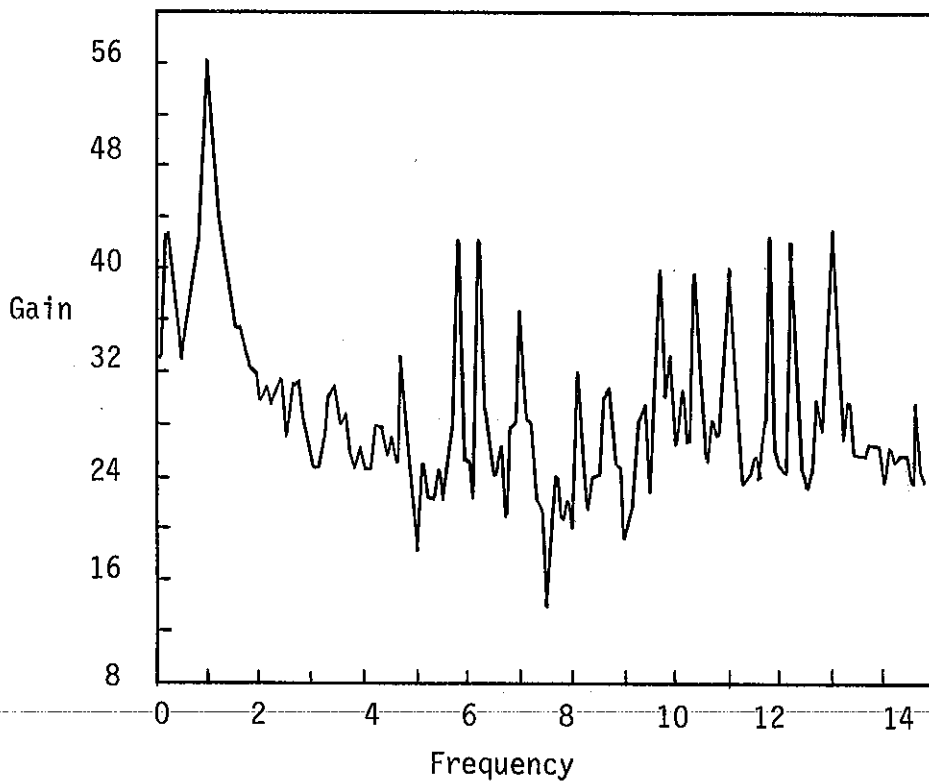


Fig. 2.6: Hard-clipped, rounded weighting, C_{30} , 7 cycles.⁽¹⁾

ציור 2.6: hard clipped, עם FIR בעל מקדמים שלמים,
 C_{30} 7 מחזורים.⁽¹⁾

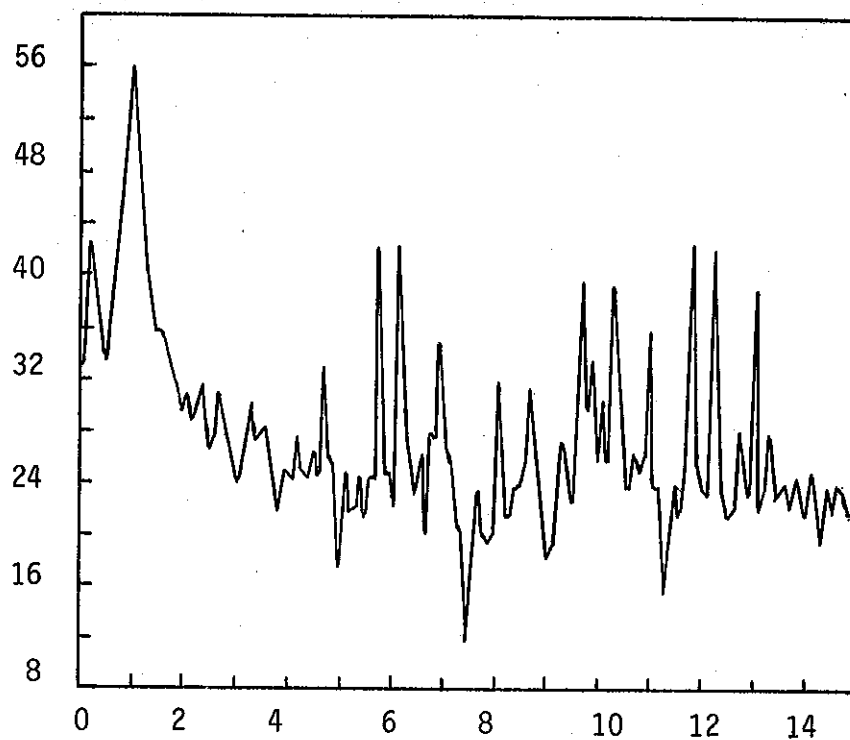


Fig. 2.7: Hard-clipped, exact weighting, C_{30} , 7 cycles⁽¹⁾.

ציור 2.7: Hard-clipped, עם FIR בעל מקדמים מדויקים, C_{30}
7 מחזוריים. ⁽¹⁾

Using a W with integer coefficients enables one to perform all the multiplications as additions, simplifying implementation and eliminating any further errors. As one expects, upon setting $\rho_2 = \bar{\rho}_1$, the Fourier coefficient of y_n at the fundamental is:

$$\begin{aligned} W(\rho_1)b_1 &= W(\rho_1) \sum_{j=2}^k \frac{\rho_1}{\rho_1 - \rho_j} = \dots \\ &= \frac{\rho_1}{\rho_1 - \rho_2} \sum_{j=3}^k \frac{\rho_1(1 - \rho_j \bar{\rho}_1)}{\rho_1 - \rho_j} = \frac{\rho_1}{\rho_1 - \rho_2} \end{aligned} \quad (2.36)$$

(2.36) gives the Fourier coefficient at the fundamental.

When W is replaced with W^I where the later is obtained through rounding off to the nearest integer the coefficients of the former. The pulse train (impulse response) resulting from W^I will have integer levels, but the truncation error will introduce higher order resonances. However, Table 2.1 shows that these are very small indeed, leaving typically about 98% of the power at the fundamental. This compares with 25% percent or less (for F_{16}, F_{24}, F_{30}) without W^I . Note, for example, F_8 . The pulse train 1,0,0,0,-1,0,0,0, has resonances at the third, fifth, and seventh harmonics. However, by simply altering this to 1,1,1,0,-1,-1,-1,0, the first appreciable resonance does not come until the seventh harmonic. In this case, use of W^I does not introduce any new levels in the pulse train. Table 2.1 gives an indication of the possibilities for various filters.

Included in Table 2.1 are the filters with memory less than 12, which provide the greatest separation between the fundamental and the first resonant harmonic, either with or without the weighing function. The asterisks(*) and daggers (†) indicate those which, for the amount of memory, have the largest possible separation without or with the weighing function.

λ (msec)	characteristic polynomial P	resonant harmonics in the band $[0, \tau^{-1}]$, aside from fundamental	with weighting function	without weighting function	first resonant harmonic due to aliasing	number of taps on filter (without weighting function)	integer-rounded weighting function τ^{-1}	A % of total power in $[0, (\pi\tau)^{-1}]$ at fundamental	B with τ^{-1}	highest power at π rejected resonance (% of fundamental)	D modulus of Fourier coefficients (in order of arguments $< \pi$)	E pulse trains	G
*1	$P_2 = \lambda^2$	none	—	—	3	1	—	100.	—	—	1	—	—
2	$P_3 = \lambda^2 + \lambda$	2	—	—	4	2	—	100.	—	—	.98	—	—
2	$P_4 = \lambda^2 + \lambda$	3	—	—	5	1	—	100.	—	—	.5	—	—
*2	$P_6 = \lambda^2 + \lambda$	5	—	—	7	2	—	100.	—	—	1.73	—	—
4	$P_8 = \lambda^2 + \lambda$	3, 5, 7	—	—	9	1	$1 + \lambda + \lambda^2$	50.	97.1	2.9	all .25	.60, .10	$1^2 0-1^2 10$
4	$P_{12} = \lambda^2 + \lambda$	5, 7, 11	—	—	13	2	$1 + 2\lambda + \lambda^2$	50.	99.5	.5	all .29	1.08, .08	$12^2 10-1^2 2^2 10$
6	$P_9 = \lambda^2 + \lambda$	2, 4, 5, 7, 8	—	—	10	2	$1 + 2\lambda + \lambda^2 + 2\lambda^3 + \lambda^4$	33.3	92.7	7.8	all .19	.85, .04, .24	$121^2 1^2 2^2 10$
6	$P_{18} = \lambda^2 + \lambda$	5, 7, 11, 13, 17	—	—	19	2	$1 + 2\lambda + 3\lambda^2 + 2\lambda^3 + \lambda^4$	33.3	99.6	.3	all .19	7.6, .04, .06	$123^2 210 \rightarrow$
8	$P_{15} = \lambda^2 + \lambda$	2, 4, 7, 8, 11, 13, 14	—	—	16	6	$1 + \lambda + \lambda^2 + \lambda^3 + \lambda^4 + \lambda^5 + \lambda^6$	53.3	98.9	.8	.33, .27, .09, .11	4.78, .51, .55, .75	$123^2 21-1^2 2^2 3^2 2-10$
8	$P_{16} = \lambda^2 + \lambda$	3, 5, 7, 9, 11, 13, 15	—	—	17	1	$1 + 2\lambda + 2\lambda^2 + 3\lambda^3 + 2\lambda^4 + 2\lambda^5 + \lambda^6$	25.	98.0	1.8	all .13	1.23, .02, .06, .17	$12^2 2^2 10 \rightarrow$
8	$P_{24} = \lambda^2 + \lambda$	5, 7, 11, 13, 17, 19, 23	—	—	25	2	$1 + 2\lambda + 3\lambda^2 + 3\lambda^3 + 3\lambda^4 + 2\lambda^5 + \lambda^6$	25.	99.5	.3	all .14	1.97, .05, .09, .11	$123^2 4^2 3^2 210 \rightarrow$
*8	$P_{30} = \lambda^2 + \lambda$	7, 11, 13, 17, 19, 23, 29	—	—	31	6	$1 + 3\lambda + 5\lambda^2 + 5\lambda^3 + 5\lambda^4 + 3\lambda^5 + \lambda^6$	6.	98.4	1.0	.11, .09, .27, .33	2.41, .04, .19, .24	$123^2 54^2 4^2 5^2 210 \rightarrow$

TABLE 2.1⁽¹⁾⁽¹⁾ 2.1 טבלה

For utilization with a "hard-clipper" (which has all odd harmonics), F_3 , F_9 and F_{15} are included. Although they resonate at all even harmonics.

The columns to the right of the double line all deal with the integer - rounded transfer function W^I . Columns A and B give $|b_1|^2 / \sum_{i=1}^{k/2} |b_i|^2$ and $|b_1 W^I(\rho_1)|^2 / \sum_{i=1}^{k/2} |b_i W^I(\rho_i)|^2$ as a percent, respectively, where b_i is the Fourier coefficient of the sequence h_n at the root ρ_i .

Column C gives $(\max_{2 \leq i \leq k/2} |b_i W^I(\rho_i)|^2) / |b_1 W(\rho_1)|^2$ as a percent.

The roots ρ_i ($i=1, \dots, k/2$) are assumed to be in order of ascending argument $\angle \rho_i$ (so ρ_1 is the fundamental).

Columns D and E give the moduli of the Fourier coefficients b_i and $b_i W^I(\rho_i)$ of the sequence x_n and y_n , respectively.

Columns F and G give the pulse trains of x_n and y_n , respectively, with initial pulse $u_0 = 1$, $u_{n>0} = 0$. The exponent denotes repeated digit; the arrow indicates that the preceding train is followed by another identical train, but that each digit is the negative of what it was.

2.6 Computing Word Length and Additions Per Cycle (1)

To realize the cyclotomic filters in hardware with perfect arithmetic, the necessary amount of memory and adder complexity must be provided. We describe here how to estimate the word length and the rate of additions required to implement a cyclotomic filter with a weighing function. It shall be assumed that all operations are performed in binary form. The number of binary bits required to store each x_n is called the word length w of the system. For generators that produce a signal approximating a sinusoid, the word length required will depend on the accuracy of approximation

needed. When the filter is used as a tone detector, the word length required will depend on the duration of operation, since the signal level tends to build up, especially at frequencies close to any resonant frequency. The signal level, of course, does not uniquely specify the minimum word length. Even though for storing x_n we may need only w bits, it is conceivable that during the computations numbers greater in magnitude than x_n , which need more bits for storage, could arise. To perform operations in a serial-multiplexed manner it is desirable to have uniform word length for all operations in the feedback loop of the filter. Hence, the word length will have to be increased to accommodate any number encountered during the computations. However, for the filters considered in Table 2.2, it is possible to arrange the computations in such a way that the word length is determined by the maximum magnitude of x_n . In general there is a finite number of ways in which the additions involved in the filter can be arranged. By simulation of the different arrangements the word length can be determined.

There are two possible ways of implementing the cyclotomic filters as generators. The first is to generate the impulse response and use a weighting function; this is generally sufficient.

As the input is zero after the initial pulse $u_0 = 1$, the weighting function need only be used during the first $d+1$ steps of the filter. Let m be the largest number in the pulse train y_n of Table 2.1, and $[x]$ be the smallest integer larger than x . The word length necessary for perfect arithmetic is at least $w = [\lg_2 m] + 1$ and, for the filters considered here, w is also sufficient. (1 is added for a sign bit). This word length is shown in column B of Table 2.2.

However, rounding off the weighting function introduces errors in the effective initial values of the signal. If this approximation is not sufficiently good, then the initial conditions of the filter

can be set as accurately as needed, and then the filter is operated with the feedback loop alone. In particular, one can set the initial conditions of the filter such that $|x_n - \sin 2\pi n/p| < 2^{-m}$ ($n = 0, \dots, k-1$) where $\sin 2\pi n/p$ is the desired signal. One can then compute the minimum word length required by simulating the filter for one period. In all cases of interest here, the word length including sign is $(m+1)$ for $m \leq 12$. Hence, as an example, the cyclotomic filter of order 30 can generate a sequence (x_n) such that $|x_n - \sin 2\pi n/p| < 2^{-10}$ if the initial conditions are set such that $|x_n - \sin (2\pi n/p)| < 2^{-10}$ ($n=0, \dots, 7$), using a word length of 11.

To determine the number of binary additions per period of the filter (i.e., per cycle of the fundamental), one counts the number of bit additions per step. If m denotes the number of additions per step, then pmw is the number of binary additions per cycle, where p corresponds to F_p and w the word length used in the feedback loops. When the generator is implemented in the first way (using an initial pulse and the weighting function), the number of additions is shown in column C of Table 2.2 (not including those necessary in the initial $d+1$ steps for the weighting function).

When the generator is implemented in the second way (setting the initial conditions, the number of additions can be computed by multiplying the value in column C by w/w' , where w is the word length chosen and w' is the corresponding word length from column B.

When the filter is used as a detector, we assume that the input to the filter is a sequence which only assumes the values ± 1 . This is true, for example, when the analog signal to be detected is either hard clipped or delta modulated. In these cases, it is

advantageous to apply the weighing function to the input u_n rather than to the sequence x_n ; since, in general, x_n can assume many values other than ± 1 computations involving the weighing function are simplified if they are performed on the input. In fact applying the weighing function to the input is so simple arithmetically that it can be implemented with a ROM. On the other hand, if a ROM is not used and one wishes to save on computations by checking the threshold only in the last cycle of the filter (with respect to its duration of operation for detection, then the weighing function is best implemented on the output of the feedback loop. Then the filter can be run during all but the last cycle, without computing the weighing function.

When the weighing function is applied to the input the filter is described by:

$$v_n = \sum_{i=0}^d c_i u_{n-i} \quad (2.37a)$$

$$x_n = \sum_{i=1}^k a_i x_{n-i} + v_n \quad (2.37b)$$

Where u_n is the input into the filter and v_n is the result of the weighing function. Fig. 2.4a describes this filter.

For the filters in Table 2.1, the effect of rounding c_i to the nearest integer is slight.

Hence, it is fortiori suitable to round off $v_n = \sum c_i u_{n-i}$ to the nearest integer. Therefore, since the only values assumed by u_i are ± 1 , it suffices to have for v_n a word length of

$$w = \lceil \lceil \lg_2 \{ \sum |c_i| \} \rceil \rceil + 1 \text{ (where } \{x\} \text{ is the integer closest to } x).$$

The sequence v_n can then assume any value between $-\{\sum |c_i|\}$ and $\{\sum |c_i|\}$. (the c_i 's are the exact coefficients of W , not W^I).

With d as in (2.37.a) and w as above implementations of the weighting function with ROM requires then $2^{d+1}w$ memory bits.

The respective values for this are shown in column D of Table 2.2.

When a bank of such tuned filters is in one receiver, all filters could use one ROM for the weighting functions.

To determine the word length for use in the feedback loop of the detector, the maximum signal level can be determined by using an input u_n of the same frequency as the resonant frequency. Since the impulse response of these filters is periodic and of the same period as the resonant frequency, the later produces the maximum signal level $\sup_{n \leq N} |x_n|$, for duration of operation N_T . Let this maximum be M . The word length required should then be at least

$[[\lg_2 M]] + 1$. For all the filters considered here, $[[\lg_2 M]] + 1$ is also sufficient. The number of M , of course, is determined by N . If the cyclotomic filter is of period p , then the filter runs through N/p periods, corresponding to N/p cycles of the fundamental. Calculations have been made for two values of N/p : 7 (the number of cycles computed in ⁽²⁾ to be necessary for touch-tone interchannel rejection), and 10 (a more uniform point of reference). Table 2.2 column E shows the word length required in the feedback loop for the indicated durations, when the weighting function is computed on the input, implemented equivalently with or without a ROM.

When there is no weighting function on the input, the word length required is shown in column F.

The binary additions per cycle for the detector is determined in the same way as for the generator; the number is pmw as defined above. These numbers are shown in columns G, H, and K of Table 2.1.

Column G shows the number of binary additions per cycle in the feedback loop when a ROM is used to implement the weighting function, applied to the input. If a ROM is not used to implement the weighting function, then the weighting function has to be computed. Since the numbers involved in the computation of the weighting function on the input are generally smaller than those in the feedback loop, the word length required for their computations are smaller. Hence, one can use two different adders, one for the weighting function and one for the feedback loop. Using this arrangement, the number of additions per cycle for calculating the weighting function is shown in column K. The number of binary additions per cycle when no weighting function is used is shown in column H. To calculate the number of additions when the weighting function is applied to the input, but a ROM is not used, add columns H and K.

Column A indicates the respective cyclotomic filters described by ϕ_i their periods.

PERIOD	GENERATOR USING IMPULSE RESPONSE		DETECTOR: 7 CYCLES						DETECTOR: 10 CYCLES					
	WORD LENGTH	ADDS/CYCLE	Word Length For (x_n)			Adds/Cycle For (x_n)			Word Length For (x_n)			Adds/Cycle For (x_n)		
			WEIGHTED INPUT	UNWEIGHTED INPUT	F	WEIGHTED INPUT	UNWEIGHTED INPUT	H	K	FOR (v_n)	WEIGHTED INPUT	UNWEIGHTED INPUT	F	K
A			D											
6	2	24	-		6	72	72	72	-		7	84	7	84
8	2	16	24		7	40	56	40	112		8	64	6	48
9	3	54	128		8	90	144	90	360		8	144	6	108
12	3	72	24		8	144	192	144	288		9	216	7	168
15	3	270	512		9	630	810	630	810		10	900	7	630
16	3	48	640		9	80	144	80	1276		10	160	6	96
18	3	108	128		9	216	324	216	1134		10	360	7	252
24	4	192	640		10	288	480	288	2160		11	528	7	336
30	4	720	768		11	1440	1980	1440	3630		11	1980	8	1440

TABLE 2.2⁽¹⁾
(1) 2.2 תב"ט

CHAPTER 3

APPLICATIONS OF CYCLOTOMIC FILTERS

3.1 Introduction

Possible uses for the cyclotomic filters have been mentioned in section 2.1. Various applications were suggested by R. Kurshan and B. Gupinath. These applications are described in this chapter. A new application proposed in this work and which was realized in hardware, is briefly described in this section. The new application is described in detail in chapters 4 to 7.

3.2 FSK⁽¹⁾

As described in chapter 3, by selecting the initial conditions of a cyclotomic filter of period p , one can approximate uniformly sampled values of a sinusoid of period p , i.e., $\sin(2\pi n/p)$. By changing the clock rate of the filter, one can shift the frequency of the sinusoid to any preassigned value. Hence, when using the filter as a generator, one can shift the clock rate to shift the frequency. This method of shifting frequencies does not introduce any "discontinuities" in the signal.

In a similar manner, when using the filter as a detector, one can shift the resonant frequency by shifting clock rate. Hence, with the same filter, one can generate and detect both tones used in a typical arrangement.

3.3 A Touch-Tone[®] Receiver-Generator (2)

The basic Touch-Tone telephone must generate tones to identify the ten basic possible inputs (1,2,...,9,0) or, in the case of augmented telephones, 12 to 16 possible inputs (including, for example, * and #). This is done by arranging the input buttons

in a grid of four rows and three or four columns. Associated with each row is one of four "low" frequencies (697, 770, 852, or 941 Hz), and associated with each column is one of three or four "high" frequencies (1209, 1336, 1477, or 1633 Hz). When a button is pushed, one low and one high frequency are simultaneously generated corresponding to the row and column in which the button is situated.

In the central office, a detector decodes the incoming pair of tones to determine which button was pushed. An incoming signal first passes through a series of tuned filters that filter out dial tones, ring tones, busy tones, and power harmonics (which have amplitude too large to be accommodated by the subsequent channel filters). Next, the signal passes through two parallel bandpass filters BPF (see Fig. 3.1) - one to reject the four high-frequency tones (low BPF) and one to reject the four low-frequency tones (high BPF). The output of each BPF passes through a hard-limiter, which convert the analog output of the BPFs into a signal which is either +1 or -1, depending on whether the analog signal is nonnegative or negative, respectively.

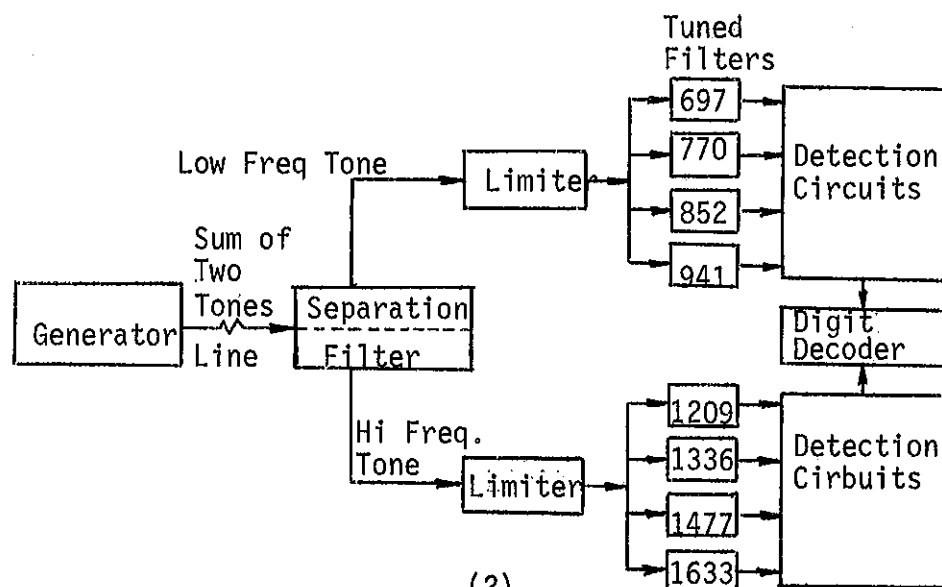


Fig. 3.1: General receiver (2).

(2)
ציור 3.1: מקלט כללי.

The channel filters which follow the hard-limiters are identical cyclotomic filters, F_p . The cyclotomic filter for each channel has as its input the output of the hard-limiter sampled at a rate p times the channel frequency, where p is the period of the cyclotomic filter used. This requires clock pulses of different frequencies for the different channels.

The channel filters are run periodically for an interval of time inversely proportional to the channel frequency, called the interval of operation. At the beginning of each such interval, the filters are set to zero. The magnitude of the output of each of the filters is compared with a fixed threshold, when the magnitude exceeds this level, a tone corresponding to this frequency is assumed to be present. The length of the interval of operation is dependent on the permissible error. An interval of operation corresponding to seven cycles of the channel frequency was found to be sufficient. This corresponds to 10ms for the channel corresponding to the lowest Touch-Tone frequency, 697 Hz. Hence, if the 697 Hz channel tone is present for the required 40msec (typical time allowed for a single detection) then in at least three consecutive intervals the tone will produce a signal above the threshold. For higher frequencies the interval of operation is shorter.

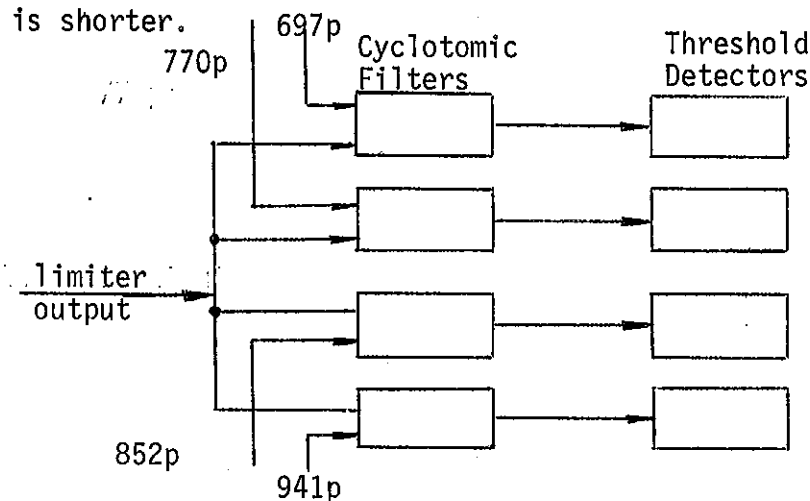


Fig. 3.2: Channel filters of the low group. (2)

(2) ציור 3.2: מסנני הערוץ של קבוצת התדר הנמוך.

By synchronizing the intervals of operation of all channels, testing is made for the simultaneous presence of a high tone and a low tone. When a high tone and a low tone are each present for three consecutive intervals, a valid Touch-Tone signal is assumed to be present. The digit corresponding to a pair of tones is decoded. C_6 is suggested for use as the cyclotomic channel filter. For more details refer to ⁽²⁾

3.4 Periodic Sequence Generators (3,4)

Digital periodic sequences are usually generated by shift registers with feedback using mod 2 arithmetic. Periodic sequence generators based on cyclotomic filters use ordinary arithmetic. Furthermore, the feedback is obtained from taps which are ± 1 or 0.

The general model of an array of shift registers used to generate a periodic sequence (y_n) can be described as follows: Let \bar{x}_n be the vector whose components denote the states of the shift register array at time n . The dimension k of \bar{x}_n is the number of delay stages available, which will be referred to as the memory. The periodic sequence (y_n) is produced by some transversal operation h on \bar{x}_n .

Fig. 3.3 gives the schematic for a linear recursive algorithm using k stages.

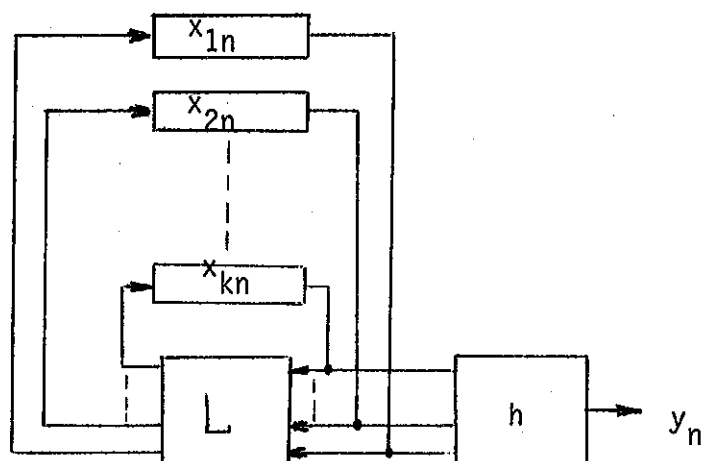


Fig. 3.3: Schematic linear recursive algorithm.

ציור 3.3: תאור סכמתי של אלגוריתם לינארי רקורסיבי.

The equations that describe the system are:

$$\bar{x}_{n+1} = L \bar{x}_n \quad (3.1a)$$

$$y_n = h(x_n) \quad (3.1b)$$

We assume that L is periodic, i.e., there exists a smallest integer p such that $\bar{x}_n = \bar{x}_{n+p}$ for all initial states.

It was shown in ⁽³⁾ that introducing nonlinear feedback cannot increase the period (or for given period, reduce the memory).

Here L is a $k \times k$ matrix. To simplify mechanization of the recursion it is useful to restrict the elements of L to be $\pm 1, 0$. In this case for arbitrary period p there is a recursion L whose elements are $0, \pm 1$, which requires only as much memory as would be necessary, where the elements of L were allowed to be arbitrary rational numbers ⁽³⁾.

The canonical form of this recursion L is now described. Let

$$p = \prod_{i=1}^r p_i^{\epsilon_i}$$

be the canonical prime number decomposition of the period p;
if $(p,4)$, the greatest common divisor of p and 4, is not equal 2,
define L to be the matrix:

$$L = \begin{bmatrix} L_1 & & & & \\ & L_2 & & & \\ & & \ddots & & \\ & & & 0 & \\ & 0 & & & \\ & & & & L_r \end{bmatrix} \quad (3.2a)$$

$$L_i = \begin{bmatrix} 0 & 1 & 0 & \dots & \dots & 0 \\ 0 & 0 & 1 & 0 & \dots & \dots & 0 \\ 0 & 0 & 0 & 0 & 1 & 0 & \dots & \dots & 0 \\ 0 & 0 & \dots & \dots & \dots & 0 & 1 \\ \alpha_{k_i} & \alpha_{k_i-1} & \dots & \dots & \dots & \alpha_1 & 1 \end{bmatrix} \quad (3.2b)$$

where for $k \equiv k_i$, $q \equiv p_i$, $\epsilon \equiv \epsilon_i$ and -

$$C(\lambda) = \lambda^{q-1} + \lambda^{q-2} + \dots + 1$$

$$\lambda^k = \sum_{i=1}^k \alpha_i \lambda^{k-i} = C(\lambda^q)^{\epsilon-1} \quad (3.3)$$

Since all the coefficients of $C(\lambda)$ are 1, the α_j 's are -1,0. The recursion associated with each L_i is then of the form:

$$y_n = \sum_{j=1}^k \alpha_j y_{n-j} \quad (3.4)$$

where $k = q^{\epsilon}(q-1)$, hence, combining the r recursions the minimum memory required to generate sequences of period:

$$p = \prod_{j=1}^r p_j^{\epsilon_j}, \quad (4, p) \neq 2$$

is:

$$\sum_{j=1}^r p_j^{\epsilon_j-1} (p_j-1) \quad (3.5)$$

This expression enables one to compute the maximum period achievable with a given memory.

Table 3.1 shows the maximum period sequence that can be generated as the function of memory.

If p equals 576 by (3.5) one obtains the minimum memory to be 38, in the same way if $p = 577$, then $k = 576$. Hence, a judicious choice of period could effect a substantial saving of memory.

When $(p, 4) = 2$, let $p = 2^{\epsilon_1} p_1^{\epsilon_1} \dots p_r^{\epsilon_r}$ be the canonical prime decomposition of p . Then the canonical form of L is identical to the previous except for the (say) first block which is now replaced by the cyclotomic filter $C(-\lambda^{p_1^{\epsilon_1}-1})$ which has coefficients 0, ± 1 .

Memory (k)	Maximum Period (p = M _k)	Memory (k)	Maximum Period (p = M _k)
1	2	68	17907120
2	6	70	24504480
4	12	72	38798760
6	30	74	58198140
8	60	76	116396280
10	120	80	232792560
12	210	84	281801520
14	420	86	314954640
16	840	88	465585120
18	1260	92	698377680
20	2520	94	892371480
24	5040	96	1338557220
26	9240	98	2677114440
28	13860	102	5354228880
30	27720	108	6750984240
32	32760	110	10708457760
34	55440	114	16062686640
36	65520	118	26771144400
38	120120	122	32125373280
40	180180	124	38818159380
42	360360	126	77636318760
46	720720	128	82990547640
50	942480	130	155272637520
52	1113840	132	165981095280
54	2042040	138	310545275040
56	3063060	140	331962190560
58	6126120	142	465817912560
60	6846840	144	497943285840
62	12252240		
64	13693680		

Table 3.1.: Maximum period vs. memory. (4)°

(4) ציור 3.1: מחזור מקסימלי כנגד גודל הזכרון.

The minimum memory again, is given by (3.5).

Equation (3.1b) describes the operations on the vector output of the recursion L which transform this to the (scalar) output of the number generator. Periodicity of the output is guaranteed, of course, independent of h, by the periodicity of L. The only standing requirement on h is that it does not decrease the effective period of the recursion i.e., that the period of the output y_n be the same as the period of the input $\bar{x}_n = L^n \bar{x}_0$.

When h is essentially a function of single outputs from each array of shift registers of relatively prime periods (as is the case in the above realization when h depends on only one component from each L_i), then h (linear) will preserve the period of (\bar{x}_n) if only all its coefficients are non zero.

Example 3.1:

Suppose that the amount of available memory is 34 stages. In Table 3.1, one can find that the maximum period possible is 55440. Since the prime number decomposition of 55440 is $2^4 \cdot 3^2 \cdot 5 \cdot 7 \cdot 11$, the memory will be distributed among five shift registers corresponding to the five distinct primes, as shown in Fig. 2.11. Specifically, for example, the second shift register corresponds to the $C(\lambda)$ for $q=3$ and $\epsilon=2$: $\lambda^6 + \lambda^3 + 1$, and thus is defined by the recursion $x_{n+6} = -x_{n+3} - x_n$ (or memory 6).

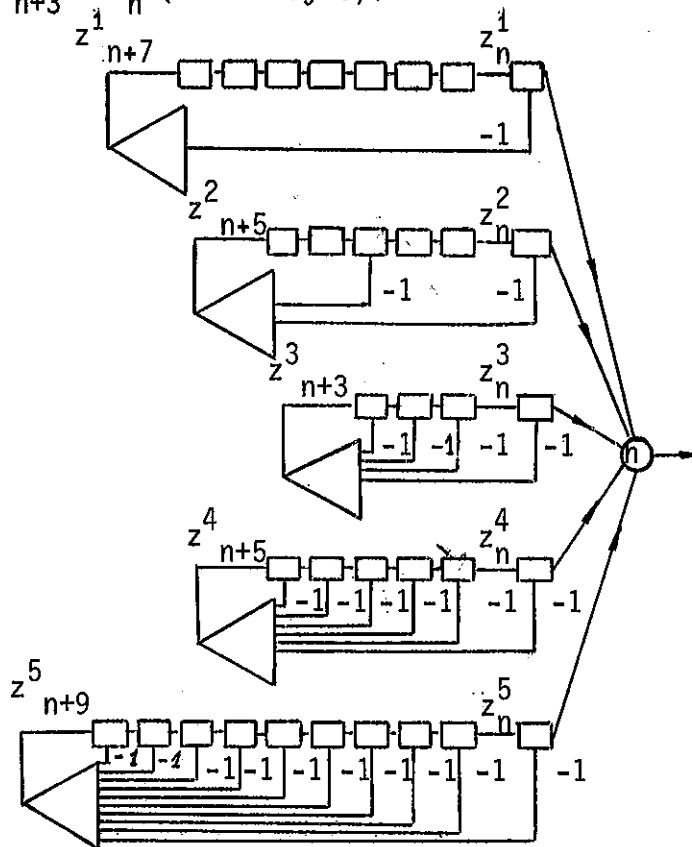


Fig. 3.4: Realization of Example 2.4.

ציור 3.4: מימוש של דוגמה 2.4.

In general, if a sequence of period p is to be constructed express p in terms of its prime number decomposition, say $p = p_1^{\epsilon_1} \dots p_r^{\epsilon_r}$. First, suppose that if one of the p_i 's is a 2, the corresponding ϵ_i is greater than 1. In this case, the sequence generator will be built from r shift registers corresponding to q (q one of the primes p_i , ϵ one of the integers ϵ_i) has $(q-1)q^{\epsilon-1}$ stages and, viewing the shift register in the direction of signal transfer (left to right in Fig. 3.4), every $q^{\epsilon-1}$ -th stage is connected to a tap with feedback coefficient -1. Thus, there are $q-1$ evenly spaced taps. If (say) $p_1^{\epsilon_1} = 2$ then (say) the first cyclotomic filter will be:

$$C_{p_1^{\epsilon_1} p_2^{\epsilon_2}}(\lambda) = C_{p_2^{\epsilon_2}}(-\lambda^{p_2^{\epsilon_2-1}})$$

3.5 A Bank of Single Tone Detectors

This is a proposed new application, dealt in detail in chapters 4-7. The system is based on the cyclotomic filters C_1, C_2, C_3, C_6 . Given a single tone of frequency f ; $f_L < f < f_H$, of constant amplitude and random phase, the system indicates in which of 64 cells of B.W. $f_H/64$ is the tone present. The system is described in chapter 4, analysed in presence of a noisy input in chapter 5, the simulation results are given in chapter 6 and the details of realization are given in chapter 7.

Measurements from the implemented CTD system are given in Chapter 8.

CHAPTER 4

THE CYCLOTOMIC TONE DETECTION SYSTEM,

PRINCIPLE OF OPERATION

4.1 Introduction

Briefly the CTD system is a single tone detector. The tone appears with constant amplitude, random phase and random frequency which is uniformly distributed in the range $0 \div f_H$. The system indicates in which of $64 (=4^3)$ cells of bandwidth $f_H/64$ is the tone present.

In a traditional bank of filters, a filter corresponds to each cell. If the tone is present in cell i , then the tone will appear in the output of the i^{th} filter, while in the output of all the other filters the tone appear attenuated.

The CTD system is not a bank of BPF's but only indicates, digitally, in which of the 64 cells is the tone present.

The system is based on the cyclotomic filters C_1, C_2, C_3 and C_6 . These filters together with C_4 are the only cyclotomic filters having a single resonant harmonic. These filters are simple to implement, since no transversal is needed, and are at most of the second order.

The tone is first converted to a complex tone, i.e., $(A \cos(2\pi ft + \phi))$ is converted to $A \exp(2\pi ft + \phi_1)$, this is done to eliminate the effect of the random phase, as will be explained.

Referring to Fig. 4- 9, there are three stages, Fig. 4-9a to Fig. 4- 9c.

At the first stage, Fig. 4-9a., the complex tone is sampled and converted by an A/D with sampling frequency $f_s = 4f_H$. The system detects in which of the four quadrants of bandwidth $f_H/4$ is the tone present. The filters C_1, C_2, C_3, C_6 can not perform the above task. C_1 and C_6 cover the first and third quadrants respectively, thus leaving the second and fourth quadrants uncovered.

This problem is solved by covering the second quadrant with $C_3(j^k)$ which means multiplying the sampled complex tone by j^k and operating C_3 . The fourth quadrant is covered with $C_2(j^k)$. This method was suggested in ⁽¹¹⁾, multiplying the sampled complex tone by $(j)^k$ is equivalent to shifting the tone's frequency by $f_s/4$ to the right and the resulting tone can be detected under C_3 or C_2 in the case of $C_3(j^k)$ or $C_2(j^k)$ respectively.

At the second stage the CTD system is operated with a sampling frequency of $f_{c_2} = f_H$. Fig. 4.9b shows how in this stage the band $(0, f_H)$ is² covered by 16 filters. If at the first stage the tone is detected in the second quadrant (the tone's frequency f satisfies $f_H/4 < f < f_H/2$), then at the second stage the four filters under this quadrant are operated. ($C_2(j^k), C_3C_3(j^k), C_2$). Continuing in this way for three stages it is possible to tell in which of 64 cells of bandwidth $f_H/64$ is the tone present.

At each stage four filters are operated. The four filters receive the same input, for a finite time; N/f_{c_s} . (N samples of the input; $s = 1, 2, 3$).

The outputs of the four filters after N samples are the basis for the decision in which of the four filters is the tone present.

In the implemented system in each stage the operation of the four filters is repeated an odd number of times and a majority decision rule is used. Repetitions are performed with new data and are

intendent for improving the noise immunity of the system. For example if at the first stage there are 31 repetitions and if at least in 16 repetitions the tone is detected in the third filter (C_6), then it is decided that the tone's frequency satisfies $\frac{1}{2}f_H < f < 3/4f_H$.

Section 4.2 gives a description of the digital filters used in the system. Section 4.3 gives the response of the filters to a sine wave, in this section it is also explained why a complex tone should be used. In 4.3.1 the response of C_1 and C_2 to a complex tone is developed.

In 4.3.2 the response of C_3 and C_6 to a complex tone is developed. On the first reading, 4.3.1. and 4.3.2 can be omitted, but refer to Fig. 4.5 and 4.6.

Section 4.4 explains that shifting the input frequency is equivalent to shifting the filters response without changing the input's frequency.

Section 4.5 explains the principle of operation of the CTD system.

4.2 Description of the Digital Filters in the CTD System

The system is based on the following cyclotomic filters:

The first is:

$$C_1(x) = x-1 \quad (4.1)$$

With the corresponding difference equation:

$$x_n = x_{n-1} + u_n \quad (4.2)$$

The second,

$$C_2(x) = x+1 \quad (4.3)$$

$$x_n = -x_{n-1} + u_n \quad (4.4)$$

The third,

$$C_3(x) = x^2 + x + 1 \quad (4.5)$$

$$x_n = -x_{n-1} - x_{n-2} + u_n \quad (4.6)$$

The fourth,

$$C_6(x) = x^2 - x + 1 \quad (4.7)$$

$$x_n = x_{n-1} - x_{n-2} + u_n \quad (4.8)$$

Fig. 4.1 gives the block realization of C_1 and C_2 .

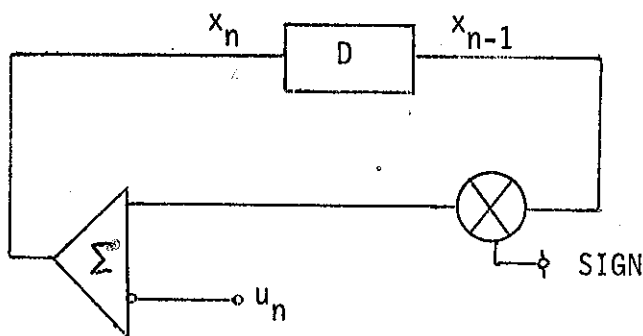


Fig. 4.1: Realization of C_1 (SIGN = 1) or C_2 (SIGN = -1).
ציור 4.1: מימוש בלוקים של C_1 (SIGN=1) או C_2 (SIGN = -1)

In the implemented system C_1 or C_2 are needed one at a time.

Fig. 4.1 shows that by a suitable choice of SIGN either C_2 (SIGN=1) or C_2 (SIGN = -1) can be chosen.

Fig. 4.2 gives the block realization of C_3 and C_6 .

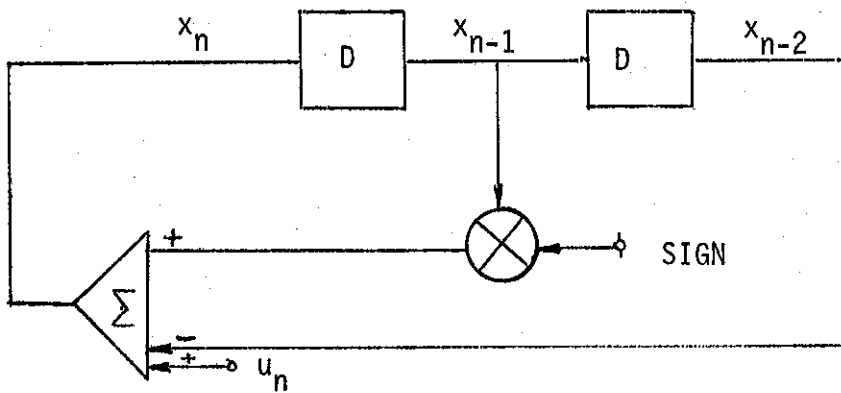


Fig. 4.2: Block realization of $C_3(\text{SIGN} = -1)$ or $C_6(\text{SIGN} = 1)$.
 ציור 4.2: מימוש בלוקים של $C_3(\text{SIGN} = -1)$ או $C_6(\text{SIGN} = 1)$.

In the implemented system C_3 or C_6 are needed one at a time.
 Fig. 4.2 shows that by a suitable choice of SIGN either $C_3(\text{SIGN} = 1)$ or $C_6(\text{SIGN} = -1)$ can be chosen.

4.3 The Response of the Filters to a Sine Wave (Tone)

Let the impulse response of a cyclotomic filter be:

$$\{h_k\}_{k=0}^{\infty} \quad \text{then:}$$

$$x_n = \sum_{k=0}^n u_k h_{n-k} \quad (4.9)$$

where:

u_k = is the input at instant k and
 $u_k = 0$ for $k < 0$

x_n = is the output at instant n
 u_k is given by:

$$u_k = A \cos \left[\frac{2\pi f}{f_s} k + \phi \right] \quad (4.10)$$

$$k = 0, 1, \dots, \infty$$

where:

$A \triangleq$ Amplitude of the tone

$f \triangleq$ the tone's frequency

$f_s \triangleq$ the sampling frequency

$\phi \triangleq$ the phase shift of the tone, a random variable.

To compute x_n a complex input is applied and the real part of the output is taken. Let θ be the angular frequency given by:

$$\theta = \frac{2\pi f}{f_s} \quad (4.11)$$

then:

$$\begin{aligned} x_n &= \operatorname{Re} \left(\sum_{k=0}^n A e^{j(k\theta + \phi)} h_{n-k} \right) \\ &= \operatorname{Re} \left(e^{j\phi} \sum_{k=0}^n A e^{jk\theta} h_{n-k} \right) \end{aligned} \quad (4.12)$$

Let:

$$\alpha_n(\theta) + j\beta_n(\theta) \triangleq \sum_{k=0}^{\infty} A e^{jk\theta} h_{n-k} \quad (4.13)$$

α_n and β_n are real for all n .

hence:

$$x_n = \alpha_n(\theta) \cos \phi - \beta_n(\theta) \sin \phi =$$

$$= \sqrt{\alpha_n^2(\theta) + \beta_n^2(\theta)} \sin \left[\tan^{-1} \frac{\alpha_n(\theta)}{\beta_n(\theta)} - \phi \right] \quad (4.14)$$

For a given $f(\theta)$ and n , x_n is strongly dependent on ϕ . Since ϕ is a random variable uniformly distributed in the interval $(0, 2\pi)$, threshold detection can't be used, and the cyclotomic filters are impractical.

Therefore a configuration as in Fig. 4.3 is used to cancel the effect of ϕ .

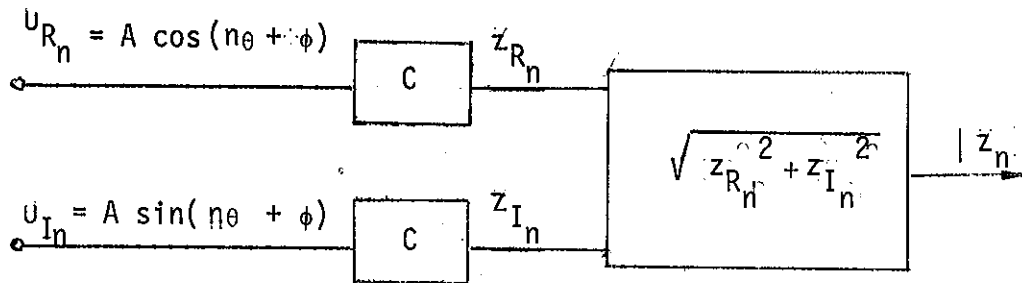


Fig. 4.3: Cyclotomic filter realization with a complex input.
צירור 4.3: מימוש של מסנן ציקלוטומי עם כניסה קומפלכסית.

By (4.12) z_n is given by:

$$z_n = A e^{j\phi} \sum_{k=0}^n e^{jk\phi} h_{n-k}$$

hence:

$$|z_n| = A \left| \sum_{k=0}^n e^{jk\theta} h_{n-k} \right| \quad (4.15)$$

From (4.15) it is clear that using the realization of Fig. 4.3 the dependence of the output on ϕ is eliminated.

In the implemented system u_R and u_I are obtained from $u(t)$ by analog linear networks ⁽¹²⁾. The method is explained in Chapter 7.

4.3.1* The Response of C_1 and C_2 to a Complex Input

The impulse response of C_1 and C_2 is obtained by applying $u_n = \delta_n$ to (4.2) and (4.4) respectively. One obtains:

$$\text{For } C_1, \quad h_n = 1 \quad n \geq 0 \quad (4.16)$$

$$\text{For } C_2, \quad h_n = (-1)^n \quad n \geq 0 \quad (4.17)$$

by (4.15) one obtains:

$$z_{C_1}(n, \theta) = A \left| \sum_{k=0}^n e^{jk\theta} \right| =$$

$$\left| z_{C_1}(n, \theta) \right| = A \left| \frac{e^{j\theta(n+1)} - 1}{e^{j\theta} - 1} \right|$$

$$\left| z_{C_1}(n, \theta) \right| = A \left| \frac{\sin \theta \frac{n+1}{2}}{\sin \frac{\theta}{2}} \right| \quad (4.18)$$

* This section can be omitted on first reading.

Similarly for C_2 one obtains:

$$|z_{C_2}(n, \theta)| = A \left| \frac{\sin \frac{(\theta + \pi)(n+1)}{2}}{\sin \left(\frac{\theta + \pi}{2} \right)} \right| \quad (4.19)$$

Note: For $|z_{C_1}(n, 0)|$ and $|z_{C_2}(n, \pi)|$ one has to take the limit (the result is $n+1$ for the two cases).

From (4.18) and (4.19):

$$|z_{C_2}(n, \theta)| = |z_{C_1}(n, \theta + \pi)| \quad (4.20)$$

Hence: $|z_{C_2}(n, \theta)|$ can be obtained from $|z_{C_1}(n, \theta)|$ by shifting θ, π rad.

4.3.2* The Response of C_3, C_6 to a Complex Input

Applying $u_n = \delta_n$ to (4.6) and (4.8) one obtains:

$$\text{for } C_3: h_n = \{1, -1, 0, \dots\} \quad (4.21)$$

$$\text{for } C_6: h_n = \{1, 1, 0, -1, 1, 0, \dots\} \quad (4.22)$$

h_n of $C_3(C_6)$ is periodic of period 3(6) respectively.

obviously:

$$h_{C_3}(n) = h_{C_6}(n)(-1)^n \quad (4.23)$$

* This section can be omitted on first reading.

From (4.15) one obtains:

$$|z_{C_3}(n, \theta)| = \left| \sum_{k=0}^n e^{jk\theta} h_{C_3}(n-k) \right| \quad (4.24)$$

and:

$$|z_{C_6}(n, \theta)| = \left| \sum_{k=0}^n e^{jk\theta} h_{C_6}(n-k) \right| \quad (4.25)$$

From (4.23) one concludes that

$$|z_{C_3}(n, \theta)| = |z_{C_6}(n, \theta + \pi)| \quad (4.26)$$

Hence, we can have $|z_{C_3}(n, \theta)|$ from $|z_{C_6}(n, \theta)|$ by shifting θ π radians.

To find an explicit expression for $|z_{C_3}(n, \theta)|$ two cases are considered:

Case 1: $n = 3m$ or $3m-1$

Rewriting (4.25):

$$\begin{aligned} |z_{C_3}(n, \theta)| &= A \left| \sum_{k=0}^n e^{jk\theta} h_{n-k} \right| = \\ &= |h_0 e^{jn\theta} + h_1 e^{j(n-1)\theta} + \dots + h_n| \end{aligned}$$

From (4.21) one concludes that $h_{3m-1} = 0$, hence:

$$z_{C_3}(3m-1, \theta) = z_{C_3}(3m-2, \theta),$$

therefore it is enough to compute $|z_{C_3}(n, \theta)|$ for $n = 3m-2$

$$\begin{aligned}
 |z_{C_3}(n, \theta)| &= A |(e^{jn\theta} - e^{j(n-1)\theta}) + (e^{j(n-3)\theta} - e^{j(n-4)\theta}) \\
 &\quad + \dots + (e^{j\theta} - 1)| = \\
 |z_{C_3}(n, \theta)| &= A |e^{j\theta} - 1| [e^{j(n-1)\theta} + e^{j(n-4)\theta} + \dots + \\
 &\quad + e^{j3\theta} + 1] \\
 |z_{C_3}(n, \theta)| &= A \left| (e^{j\theta} - 1) \frac{1 - e^{j3m\theta}}{1 - e^{j3\theta}} \right| = \\
 &= 2A \left| \sin \frac{\theta}{2} \frac{\sin \frac{3m}{2} \theta}{\sin 1.5\theta} \right| \quad (4.27)
 \end{aligned}$$

$n = 3m$ or $3m-1$, $m = 1, 2, \dots$

From (4.26) and (4.27) one obtains:

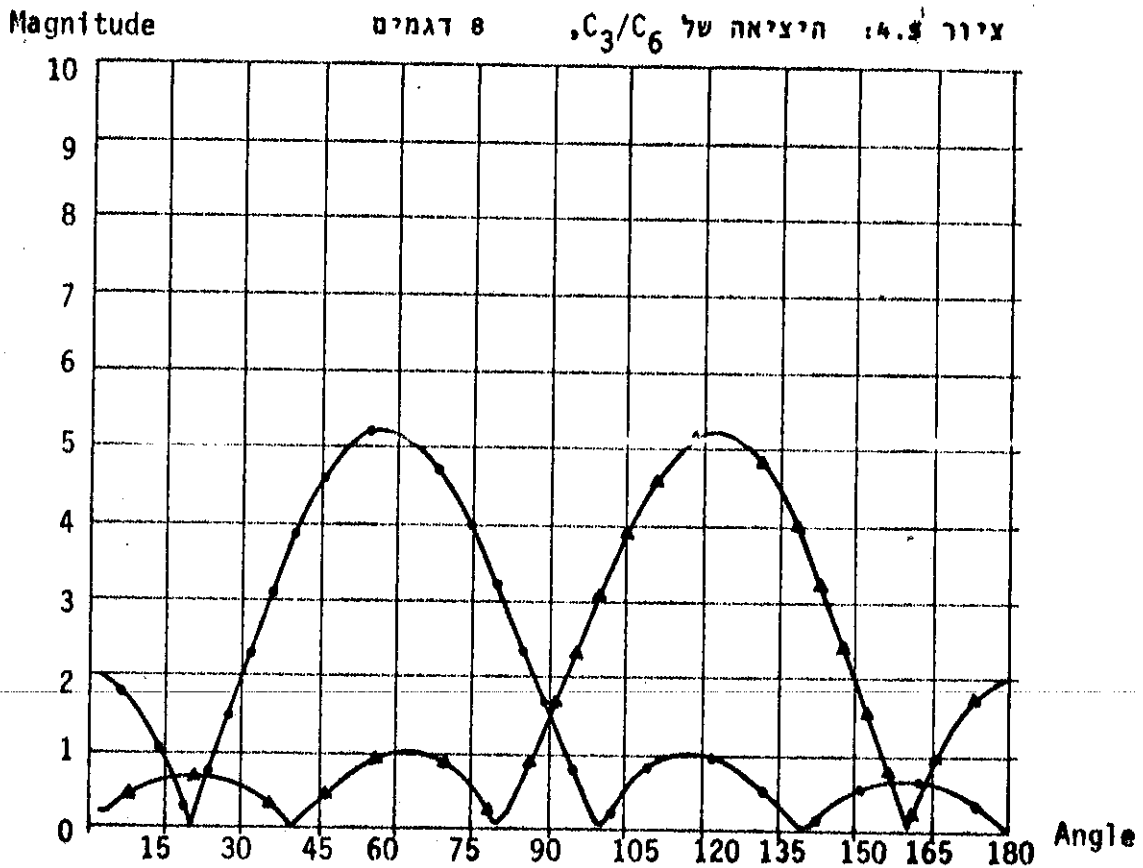
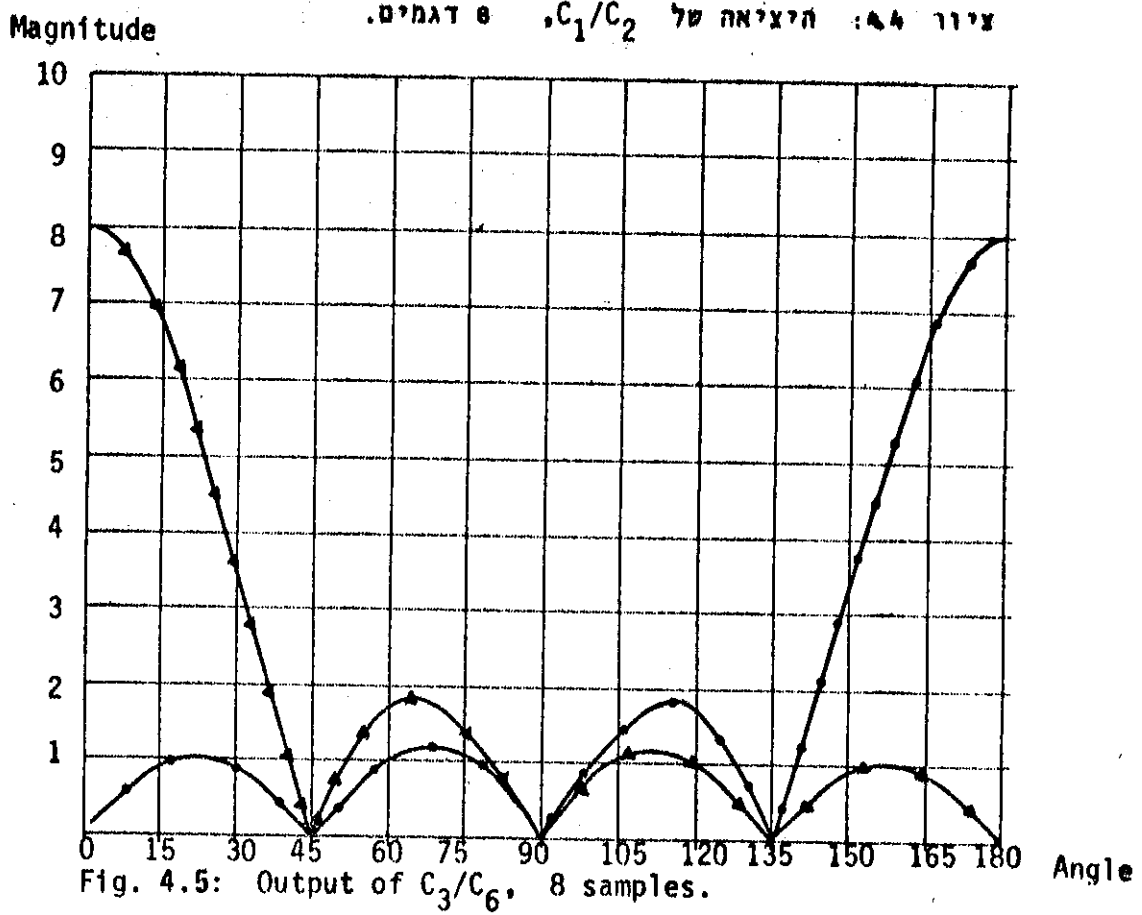
$$\begin{aligned}
 |z_{C_6}(n, \theta)| &= 2A \left| \sin \frac{\theta+\pi}{2} \frac{\sin \frac{3m}{2} (\theta+\pi)}{\sin 1.5 (\theta+\pi)} \right| \quad (4.28) \\
 n &= 3m \text{ or } 3m-1, \quad m = 1, 2, \dots
 \end{aligned}$$

Note: $|z_{C_3}(n, \frac{2}{3}\pi)|$ and $|z_{C_6}(n, \frac{\pi}{3})|$ are found taking the limit.

Case 2: $n = 3m-2$

Similarly to case one, one can obtain:

Fig. 4.4: Output of C_1/C_2 , 8 samples.



$$|z_{C_3}(n, \theta)| = A \left| 2e^{-j\frac{n-2}{2}\theta} \frac{\sin \frac{\theta}{2} \sin \frac{n-2}{2}\theta}{\sin 1.5\theta} + 1 \right| \quad (4.29)$$

$|z_{C_6}(n, \theta)|$ is obtained by (4.26).

Fig. (4.4) gives plots of $|z_{C_3}(7, \theta)|$ and $|z_{C_2}(7, \theta)|$, Fig.(4.5) gives plots of $|z_{C_3}(7, \theta)|$ and $|z_{C_6}(7, \theta)|$.

The plots of Fig. (4.4) and (4.5) are for $n=7$ (8 samples of the input). In the implemented system each filter runs for 8 samples of the input, a decision is made and the filters are reset.

From section (4.3) one concludes that operating $C_1(C_6)$ is equivalent to operating $C_2(C_3)$ with the complex input multiplied by $(-1)^n$.

4.4 An Equivalent of Shifting the Input Frequency

This section explains the meaning of $C(j^k)$.

In general the input can be multiplied by $e^{jn\alpha}$ where α is a given angle. α corresponds to a frequency shift: $\Delta f = \alpha f_s / 2\pi$. This is equivalent to shifting the filter's response by $-\alpha$ without changing the input frequency.

In the implemented system a shift of $\alpha = \frac{\pi}{2}$ is applied. $C(j^k)$ means multiplying the input by j^k and operating the cyclotomic filter C .

Fig. 4.6 describes the operation of multiplying the input by j^k

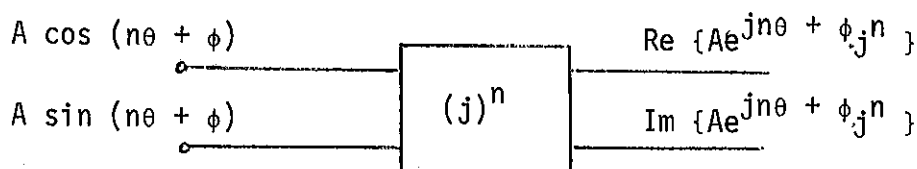


Fig. 4.6: Presentation of multiplying the input by $(j)^n$

ציור 4.6: ייצוג כפל הכניסה ב- $(j)^n$.

One can easily obtain:

n	j^n	$Ae^{j(n\theta + \phi)} j^n$	Implementation
4m	1	$A \cos(n\theta + \phi) + jA \sin(n\theta + \phi)$	
4m+1	j	$-A \sin(n\theta + \phi) + jA \cos(n\theta + \phi)$	
4m+2	-1	$A \sin(n\theta + \phi) - jA \cos(n\theta + \phi)$	
4m+3	-j	$-A \cos(n\theta + \phi) - jA \sin(n\theta + \phi)$	

Table 4.1: Expansion of the operations in Fig. 4.6.

טבלה 4.1: הרחבת הפעולות מצדור 4.6.

From Table 4.1 the implementation is very simple. For example when $n = 4m+1$ interchange the lines and multiply the imaginary line by -1. Hence the implementation incorporates operation of changing sign and/or interchanging the lines.

4.5 CTD System, Principle of Operation

The tone is first converted to a complex tone, the complex tone is converted by an A/D and multiplied by j^n .

Fig. 4.7 shows the above operations.

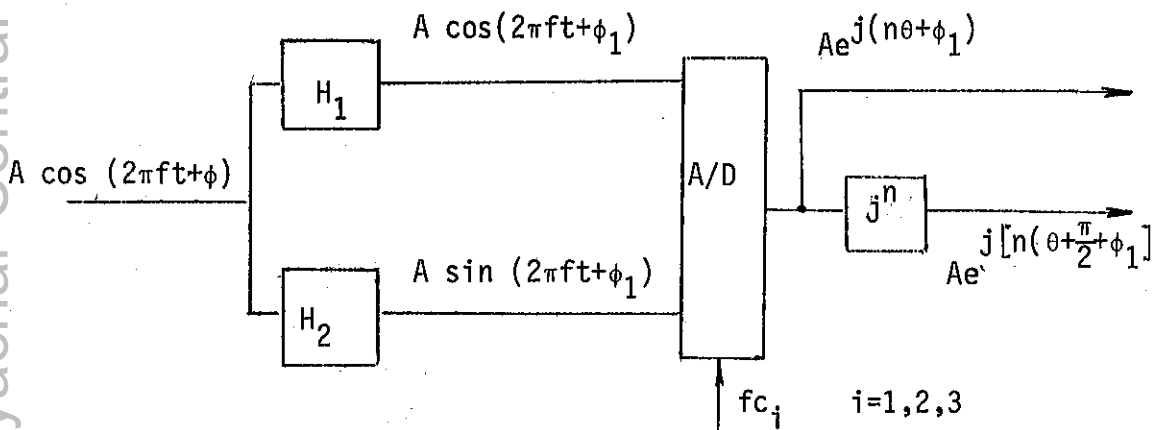


Fig. 4.7: The preprocessing of the tone.

ציור 4.7: עבוד מוקדם של הטון.

H_1 and H_2 are two all pass filters that have a phase difference of 90° , in a given band. (Their design is given in chapter 7).

Referring to Fig. (4.9), let the tone's frequency satisfy $f < f_H$. There are three stages characterized by different sampling frequencies. At stages I, II, III the sampling frequencies are $f_{C_1} = 4f_H$, $f_{C_2} = f_H$, $f_{C_3} = f_H/4$. respectively.

Stage I: Referring to Figs. 4.8 and 4.9a, the four filters $C_1, C_3(j^n), C_6, C_2(j^n)$ are operated. $C_3(j^n)$ means operating C_3 with the complex tone multiplied by j^n which is equivalent to shifting the response of C_3 $-\pi/2$ radians without changing θ .

The decision logic in stage I is as following, to decide in which of the four filters the tone appeared a threshold is attached to C_1 and C_2 . Let the threshold be TR1, then:

$$TR1 = |z_{C_1}(N-1, \theta)|_{\theta = \frac{\pi}{8}} \quad (4.30)$$

N is the number of input samples the filters are operated with.

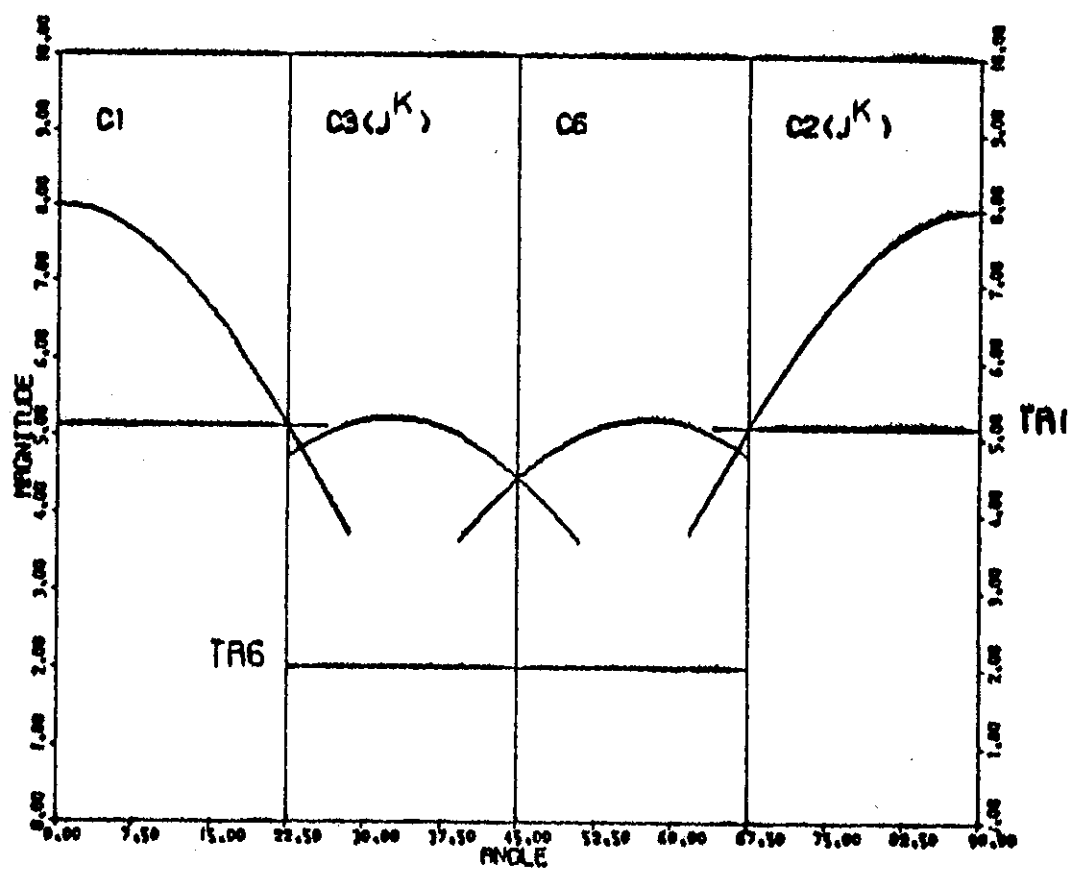


FIG. 4-8 : THE FOUR PAIRS OF FILTERS AT STAGE I
 ציור 4-8 : הצגה של הפילטרים בשלב I

For "silence detection" a threshold TR6 is attached to C_3 and C_6 .

TR6 satisfies:

$$TR6 = \frac{1}{2} |z_{C_6}(N-1, \frac{\pi}{4})| \quad (4.31)$$

The value of TR6 is a reasonable choice from noise considerations.

If the output of C_1 : $|z_{C_1}(N-1, \theta)|$ is greater than TR1 it is decided that f is in the first filter ($0 < f < f_H/4$) and the stage is terminated. If the output of $C_2(j^n)$ passes TR1 it is decided that f is in the fourth filter: $3/4 f_H < f < f_H$ and the stage is terminated.

If none of the above is satisfied and the output of $C_3(j^n)$ passes TR6 and is greater than the output of C_6 it is decided that f is in the second filter ($f_H/4 < f < f_H/2$), else if the output of C_6 passes TR6 and the output of $C_3(j^n)$ is less equal than the output of C_6 it is decided that f is in the third filter ($\frac{f_H}{2} < f < \frac{3}{4} f_H$).

If none of the above conditions is fulfilled it is decided that no signal is present.

To indicate the cell in which the tone is located a six bit register \underline{R} is used. $\underline{R} = R_6, R_5, \dots, R_1$ where R_6 is the MSB and R_1 is the LSB. After the first stage let:

$$R_6 R_5 = (\# \text{ of filter}) - 1$$

Stage II: Fig. 4.9b

At this stage the filters are operated with a sampling frequency $f_{c_2} = f_H$. There are four quadrants each consisting of four filters.

Suppose that in stage I the tone was detected at the ℓ^{th} filter, where $1 \leq \ell \leq 4$.

In stage II the four filters of the ℓ^{th} quadrant are operated and the logic of stage I is repeated.

For example suppose in Stage I a signal was detected in the third filter. In stage II the following operations are done: the filters C_2 , $C_6(j^k)$, C_3 , $C_1(j^k)$ of the third quadrant are operated.

If the output of C_2 passed TR1 then $R_4 R_3 = 00$ and this stage is terminated. If the output of $C_1(j^k)$ passed TR1 then $R_4 R_3 = 11$ and this stage is terminated.

If none of the above conditions is satisfied and the output of $C_6(j^k)$ passes TR6 and is greater than the output of C_3 then $R_4 R_3 = 01$, else if the output of C_3 passes TR6 and is greater or equal the output of $C_6(j^k)$ then $R_4 R_3 = 10$.

If none of the above conditions are fulfilled it is decided that no signal is present.

Stage III: Fig. 4.9 c

In this stage four filters are operated with sampling frequency $f_{c_3} = f_H/4$.

Fig. 4.9c consists of four replicas of Fig. 4.9b. If at stage II the signal was detected in the ℓ^{th} filter ($1 \leq \ell \leq 4$) of some quadrant (it does not matter in which quadrant) then at stage III the filters of the ℓ^{th} quadrant are operated. Under a quadrant in stage II there are 4 quadrants in stage III (i.e. one replica) and if in stage II the tone appears in the ℓ^{th} filter then under the ℓ^{th} filter appears the ℓ^{th} quadrant.

The decision logic in stage III is as in the previous stages. After completion of stage III, R_2R_1 is set and the number of cell is given by the contents of \underline{R} in binary code.

In the implemented system the operation of the four pairs of filters is repeated at each stage an odd number of times and a majority decision rule is used. Repetitions are performed with new data and are intended for improving noise immunity of the system. For example if stage I is repeated 31 times and the tone is detected in the first filter for at least 16 times, it is decided that the tone appeared in the first filter.

CHAPTER 5

DETECTION ERROR ANALYSIS OF THE CTD SYSTEM

5.1 Introduction

The input to the CTD system is a single tone of constant amplitude, random phase and with additive Gaussian noise. The CTD system indicates in which of $64(=4^3)$ cells is the tone present. As a function of signal to noise ratio at the input detection errors may occur. There are two kinds of detection errors: a signal is transmitted but is detected in the wrong cell or is not detected at all.

The purpose of this chapter is to compute the average probability of detection error, this quantity is very important since through its minimization one obtains the optimal parameters of the CTD system.

Section 2 gives definitions and expressions of the basic probabilistic quantities, such as average probability of detection error at each stage and overall probability of detection error.

In section 5.3 the error analysis of a pair of cyclotomic filters is given. The statistics of the output is found to be Rician and in practice it can be approximated by the Gaussian distribution.

In section 5.4 expressions for computing the average probability of detection error at each stage are given, without and with repetitions (cf. Ch. 4).

The next chapter gives the numerical results based on this chapter, a comparison to simulation results and a comparison to a DFT tone detection system.

5.2 Definitions of Probabilistic Quantities

The input to the CTD system is a tone whose frequency is uniformly distributed in the interval $[0, f_H]$, briefly $f \sim U[0, f_H]$. The CTD system is generally operated with L different clock frequencies: $f_{c_1} = 4f_H$, $f_{c_2} = f_H$, $f_{c_3} = f_H/4 \dots$ $f_{c_L} = f_H/4^{L-2}$. As L gets larger a finer resolution of the frequency measured is obtained. There are 4^L cells in the band $[0, f_H]$.

Let stage s correspond to f_{c_s} . At each stage an error may occur. Let \bar{P}_{e_s} be the average probability of detection error at stage s .

Let \bar{P}_D denote the average probability that the tone is correctly detected by the CTD system. Assuming each stage is statistically independent on the other stages then:

$$\bar{P}_D = \prod_{s=1}^L (1 - \bar{P}_{e_s}) \quad (5.1)$$

Let \bar{P}_E be the average probability of detection error then:

$$\bar{P}_E = 1 - \bar{P}_D \quad (5.2)$$

$$\bar{P}_E = 1 - \prod_{s=1}^L (1 - \bar{P}_{e_s}) \quad (5.3)$$

A question arises how to compute \bar{P}_{e_s} ?

Let f be the tone's frequency and θ_s the angle defined by:

$$\theta_s = (2\pi/f_{c_s})f \quad (5.4)$$

At stage s , let $P_{e_s}(\theta_s)$ be the probability of detection error as a function of θ_s , then:

$$\bar{P}_{e_s} = E\{\bar{P}_{e_s}(\theta_s)\} \quad (5.5)$$

E = Expectation

θ_s is a random variable uniformly distributed in an interval of length $\pi/2$.

5.3 Error Analysis of a Pair of Cyclotomic Filters

At each stage four pairs of filters are operated. Each pair of filters represents the equivalence of one filter receiving a complex input.

The preprocessing of the tone and a general pair of cyclotomic filters operated at stage s is shown in Fig. 5.1.

Referring to Fig. 5.1 the tone appears with additive Gaussian white noise. The tone passes through an ideal LPF: $[0, f_H]$. The purpose of the LPF is to eliminate the noise components having frequency greater than f_H . The LPF produces additive Gaussian coloured noise without changing the amplitude of the tone. H_1 and H_2 are two all pass linear networks that convert the single tone $A \sin(2\pi ft + \phi) + n(t)$ to a complex tone-
 $A \cos(2\pi ft + \phi_1) + n_R(t) + j[A \sin(2\pi ft + \phi_1) + n_I(t)]$ in a given frequency band $[f_L, f_H]$. The noisy complex tone is converted by an A/D. The samples of the noisy complex tone are multiplied by $(\alpha)^k$, where $\alpha=1$ or $\alpha=\sqrt{-1}$ ($F(j^k)$). After the multiplier α^k , two identical cyclotomic filters are operated for a finite time N/f_{c_s} . The modulus of the complex output $z_R(N-1) + jz_I(N-1)$ is found, the process terminates and the filters are reset.

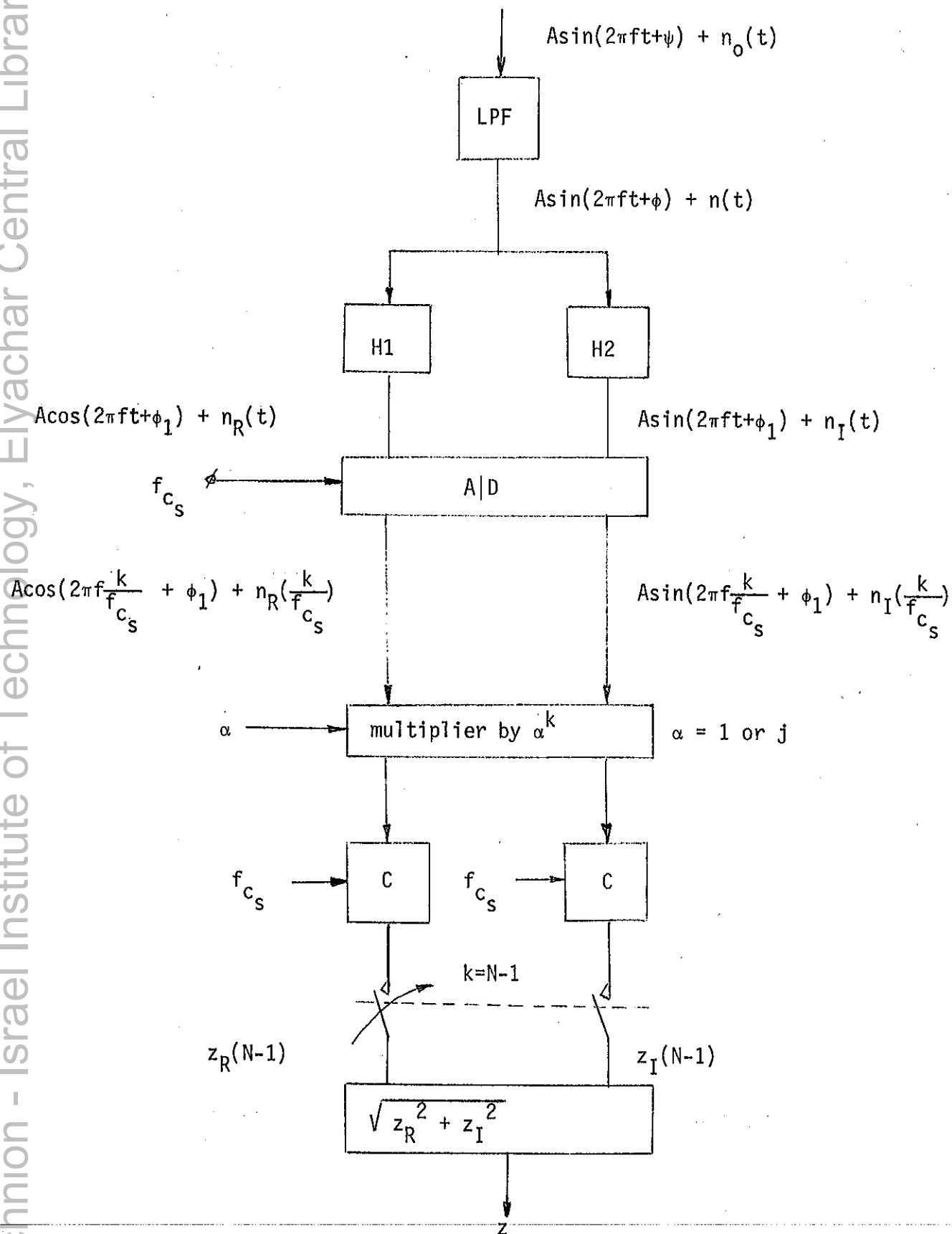


Fig. 5.1: A general pair of filters operated at stage s .

ציור 5.1: זוג מסננים כללי המופעל בשלב s .

The operation $\sqrt{z_R^2 + z_I^2}$ is very complex to implement, in the implemented CTD system a linear stochastic approximation to $\sqrt{z_R^2 + z_I^2}$ is used⁽¹⁵⁾.

Fig. 5.1 describes the principle of operating a general pair of cyclotomic filters. At each stage the complex tone is sampled with different sampling frequency f_{c_s} and the samples are processed. In the implemented CTD system the complex tone is sampled only with sampling frequency $f_{c_1} = 4f_H$. The samples are stored in a RAM. Two RAMs are operated while one Ram receives information the information of the other RAM is processed and vice versa.

The processing of the information in the suitable RAM is performed with a fast clock ($\approx 60f_H$). The different stages (f_{c_s}) are simulated, by processing samples such that consecutive^s samples have addresses differing by 4^{s-1} ($s=1,2,3$).

The theory developed in this chapter is applied to the implemented CTD system without changes.

5.3.1 The Statistics of $n(t)$

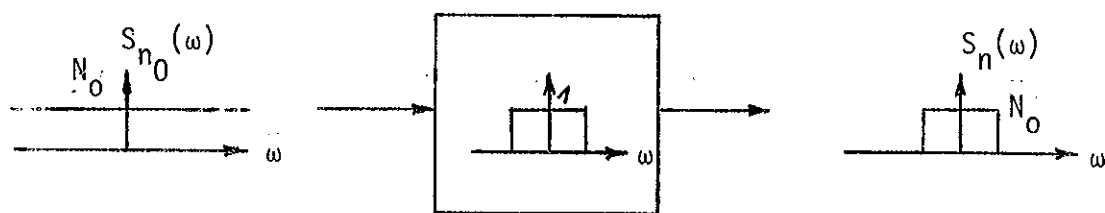


Fig. 5.2: The spectral density of $n_o(t)$ and $n(t)$.

ציור 5.2: צפיפות הספקטרום של $n_o(t)$ ו- $n(t)$.

$n_o(t)$ is Gaussian white noise with autocorrelation $R_{n_o}(\tau) = N_o \delta(\tau)$ and spectral density $S_{n_o}(\omega) = N_o$. $S_n(\omega)$ is given by:

$$S_n(\omega) = S_{n_0}(\omega) |H(j\omega)|^2 \quad (5.6)$$

$S_n(\omega)$ is plotted in Fig. 5.2.

The autocorrelation of $n(t)$ is the inverse Fourier transform of $S_n(\omega)$ and is given by:

$$R_n(\tau) = \frac{1}{2\pi} \int_{-\omega_H}^{\omega_H} N_0 e^{j\omega\tau} d\omega = \frac{N_0 \omega_H}{\pi} \frac{\sin \omega_H \tau}{\omega_H \tau} \quad (5.7)$$

Let σ_{in}^2 be the power of $n(t)$ given by $R_n(0)$

$$\sigma_{in}^2 = R_n(0) = \frac{1}{2\pi} \int_{-\omega_H}^{\omega_H} N_0 d\omega = \frac{N_0 \omega_H}{\pi} \quad (5.8)$$

Hence:

$$R_{in}(\tau) = \sigma_{in}^2 \text{sinc}(\omega_H \tau) \quad (5.9)$$

Let the signal to noise ratio at the input be defined by:

$$\text{SNR}_i = 10 \lg_{10} \frac{A^2/2}{\sigma_{in}^2} \quad (5.10)$$

5.3.2 The Statistics of $n_R(t)$ and $n_I(t)$

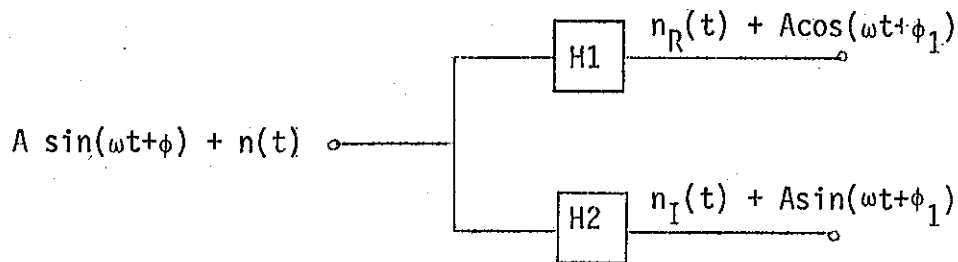


Fig. 5.3: The 90° phase shift network.

ציור 5.3: רשת הזזת הפזה ב- 90° .

Referring to Fig. 5.3 one concludes that :

$$H_1 = \begin{cases} 1e^{j(\frac{\pi}{2} + \phi_1 - \phi)} & \omega > 0 \\ -1e^{-j(\frac{\pi}{2} + \phi_1 - \phi)} & \omega < 0 \end{cases} \quad (5.11)$$

$$H_2 = \begin{cases} 1e^{j(\phi_1 - \phi)} & \omega > 0 \\ -1e^{-j(\phi_1 - \phi)} & \omega < 0 \end{cases} \quad (5.12)$$

where ϕ_1 is in general a function of ω .

The spectral density of n_R is given by:

$$S_{n_R}(\omega) = S_n(\omega) \times |H_1(j\omega)|^2 = S_n(\omega) \quad (5.13)$$

and similarly:

$$S_{n_I}(\omega) = S_n(\omega) = \sigma_{in}^2 \frac{\sin \omega_H \tau}{\omega_H \tau} \quad (5.14)$$

In the sequel the cross correlation of $n_R(t)$ and $n_I(t)$ is found:

$$S_{n_I n_R}(\omega) = S_n(\omega) \cdot H_1^*(j\omega) H_2(j\omega) = -S_{n_R n_I}(\omega) \quad (5.15)$$

From (5.11) and (5.12) it follows that:

$$H_2 H_1^* = -j \text{sign}(\omega) \quad (5.16)$$

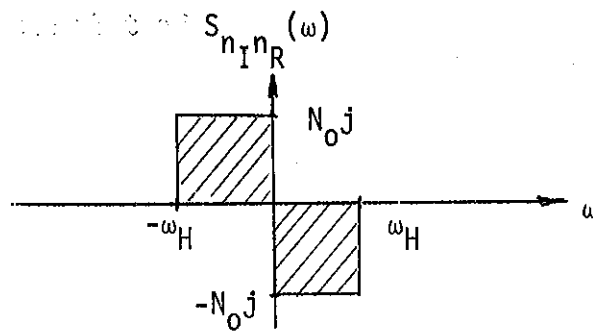


Fig. 5.4: The plot of $S_{n_I n_R}(\omega)$

צירור 5.4: הצירור של $S_{n_I n_R}(\omega)$

$$R_{n_I n_R}(\tau) = \frac{1}{2\pi} \int_{-\omega_H}^{\omega_H} S_{n_I n_R}(\omega) e^{j\omega\tau} d\omega = \frac{N_0 \omega_H}{\pi} \frac{\sin^2(\frac{\omega_H \tau}{2})}{\frac{\omega_H \tau}{2}}$$

by (5.8) it follows that:

$$R_{n_I n_R}(\tau) = \sigma_{in}^2 \frac{\sin^2 \frac{\omega_H \tau}{2}}{\frac{\omega_H \tau}{2}} \quad (5.17)$$

$$\lim_{\tau \rightarrow 0} R_{n_I n_R}(\tau) = 0 \quad \text{hence:}$$

$$E \{n_I(t) n_R(t)\} = R_{n_I n_R}(0) = 0$$

It follows that $n_I(t)$ and $n_R(t)$ are uncorrelated, and since they are Gaussian they are also statistically independent.

The CTD system is basically a digital system. In the sequel it is shown how to pass from the continuous autocorrelation and crosscorrelation functions $R_n(\tau)$ and $R_{n_I n_R}(\tau)$ to their discrete forms. At stage s the sampling frequency f_{c_s} satisfies:

$$f_{c_s} = \frac{\omega_H}{4^{s-2}} \quad (5.18)$$

$$s \in \{1, 2, \dots, L\}$$

where s is the stage number.

τ must satisfy:

$$\tau = \frac{k}{f_{c_s}} \quad (5.19)$$

Using (5.18) and (5.19) and the conversion $R(\frac{k}{f_{c_s}}) = R(k)$, one obtains that:

$$R_n(k) = R_{n_I}(k) = R_{n_R}(k) = \sigma_{in}^2 \frac{\sin \frac{k\pi 4^{s-1}}{2}}{\frac{k\pi 4^{s-1}}{2}} \quad (5.20)$$

$$R_{n_I n_R}(k) = -R_{n_R n_I}(k) = \sigma_{in}^2 \frac{\sin^2 \pi k 4^{s-2}}{\pi k 4^{s-2}} \quad (5.21)$$

Table 5.1 and 5.2 give tabulations of (5.20) and (5.21)

$s \backslash k$	0	1	2	3	4	5	6	7	8	9	10	11
1	1	$\frac{2}{\pi}$	0	$-\frac{2}{3\pi}$	0	$\frac{2}{5\pi}$	0	$-\frac{2}{7\pi}$	0	$\frac{2}{9\pi}$	0	$-\frac{2}{11\pi}$
2	1	0	0	0	0	0	0	0	0	0	0	0
3	1	0	0	0	0	0	0	0	0	0	0	0

Table 5.1: Tabulation of $R_n(k)/\sigma_{in}^2 = R_{n_I}(k)/\sigma_{in}^2 = R_{n_R}(k)/\sigma_{in}^2$

ציור 5.1: טבולציה של $R_n(k)/\sigma_{in}^2 = R_{n_I}(k)/\sigma_{in}^2 = R_{n_R}(k)/\sigma_{in}^2$

$s \backslash k$	0	1	2	3	4	5	6	7	8	9	10	11
1	0	$\frac{2}{\pi}$	$\frac{2}{\pi}$	$\frac{2}{3\pi}$	0	$\frac{2}{5\pi}$	$\frac{2}{3\pi}$	$\frac{2}{7\pi}$	0	$\frac{2}{9\pi}$	$\frac{2}{5\pi}$	$\frac{2}{11\pi}$
2	0	0	0	0	0	0	0	0	0	0	0	0
3	0	0	0	0	0	0	0	0	0	0	0	0

Table 5.2: Tabulation of $R_{n_I n_R}(k)/\sigma_{in}^2$

טבלה 5.2: טבולציה של $R_{n_I n_R}(k)/\sigma_{in}^2$

5.3.3 The Statistics of $z_R(N-1)$ and $z_I(N-1)$

Since the tone effects only the average of z_R, z_I it is assumed that the tone is not present.

In the sequel it is shown that $z_R(N-1)$ and $z_I(N-1)$ are statistically independent and have the same variance.

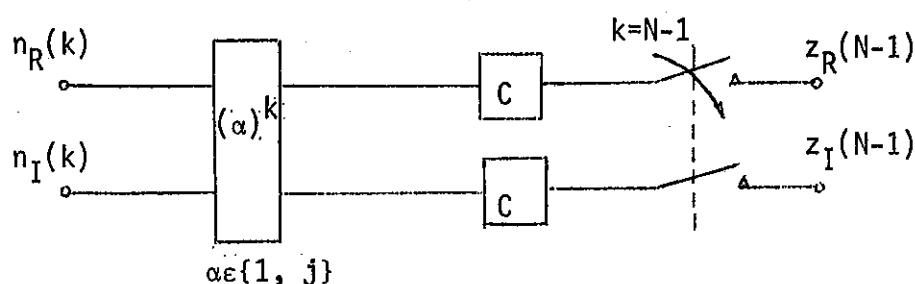


Fig. 5.5: The filters and the multiplier

ציור 5.5: המסננים והכופל.

Let us make the following definitions:

$$\underline{n}(k) \triangleq n_R(k) + jn_I(k) \quad (5.22)$$

$$\underline{z}(N-1) \triangleq z_R(N-1) + jz_I(N-1) \quad (5.23)$$

Let h_f be the impulse response of the cyclotomic filter C .

It is shown that $E\{\underline{z}^2(N-1)\} = 0$ and that

$$E\{\underline{z}^2(N-1)\} = E\{z_R^2(N-1)\} - E\{z_I^2(N-1)\} + 2jE\{z_R(N-1)z_I(N-1)\} = 0$$

hence:

$$E\{z_R^2(N-1)\} = E\{z_I^2(N-1)\} \quad (5.24)$$

and

$$E\{z_R(N-1) z_I(N-1)\} = 0 \quad (5.25)$$

From (5.24) and (5.25) it follows that $z_R(N-1)$ and $z_I(N-1)$ are uncorrelated and have the same variance.

Now to the proof that $E\{z^2(N-1)\} = 0$

$$E\{z^2(N-1)\} = E\left\{\sum_{i=0}^{N-1} h_i \alpha^{N-1-i} \underline{n}_{N-1-i} \sum_{\ell=0}^{N-1} h_\ell \alpha^{N-1-\ell} \underline{n}_{N-1-\ell}\right\}$$

$$= \sum_{i=0}^{N-1} \sum_{\ell=0}^{N-1} h_i h_\ell \alpha^{N-1-i} \alpha^{N-1-\ell} E\{\underline{n}(N-i-1) \underline{n}(N-\ell-1)\}$$

$$\begin{aligned} E\{\underline{n}(p) \underline{n}(q)\} &= E\{[n_R(p) + j n_I(p)][n_R(q) + j n_I(q)]\} \\ &= E\{n_R(p) n_R(q)\} - E\{n_I(p) n_I(q)\} \\ &\quad + j[E\{n_R(p) n_I(q)\} + E\{n_I(p) n_R(q)\}] = \\ &= R_n(p-q) - R_n(q-p) + j[R_{n_R n_I}(q-p) + R_{n_R n_I}(p-q)] = 0 \end{aligned}$$

The result follows using (5.20) and (5.21).

Using (5.24) σ_{out}^2 is defined by:

$$\sigma_{out}^2 = E\{z_R^2(N-1)\} = E\{z_I^2(N-1)\} \quad (5.26)$$

Next σ_{out}^2 is found, since:

$$\underline{z}(N-1) \underline{z}^*(N-1) = z_R^2(N-1) + z_I^2(N-1)$$

hence:

$$\sigma_{out}^2 = \frac{1}{2} E \{ \underline{z}(N-1) \underline{z}^*(N-1) \} \quad (5.27)$$

$$\sigma_{out}^2 = \frac{1}{2} E \left\{ \sum_{i=0}^{N-1} \sum_{\ell=0}^{N-1} h_i h_{\ell} \alpha^{N-1-i} (\alpha^*)^{N-1-\ell} \underline{n}(N-1-i) \underline{n}^*(N-1-\ell) \right\}$$

$$= \frac{1}{2} \sum_{i=0}^{N-1} \sum_{\ell=0}^{N-1} h_i h_{\ell} \alpha^{N-1-i} (\alpha^*)^{N-1-\ell} E \{ \underline{n}(N-1-i) \underline{n}^*(N-1-\ell) \}$$

$$\begin{aligned} E \{ \underline{n}(p) \underline{n}^*(q) \} &= E \{ [n_R(p) + j n_I(p)] [n_R(q) - j n_I(q)] \} \\ &= E \{ n_R(p) n_R(q) + n_I(p) n_I(q) \} + \\ &+ j E \{ -n_I(q) n_R(p) + n_I(p) n_R(q) \} \\ &= 2 [R_n(p-q) + R_{n_I n_R}(p-q)] \end{aligned}$$

hence:

$$\sigma_{out}^2 = \sum_{i=0}^{N-1} \sum_{\ell=0}^{N-1} h_i h_{\ell} \alpha^{N-1-i} (\alpha^*)^{N-1-\ell} [R_n(\ell-i) + j R_{n_I n_R}(\ell-i)] \quad (5.28)$$

For $s=2,3$ it is simple to find σ_{out}^2 since by (5.20) and (5.21)

$$R_{n_I n_R}(k) = 0 \text{ for all } k \text{ and } R_{n_I}(k) = \delta(k) \cdot \sigma_{in}^2.$$

hence for all the filters C :

$$\sigma_{out}^2 = \sigma_{in}^2 \sum_{i=0}^{N-1} h_i^2 \text{ for } S=2,3 \quad (5.29)$$

For $s=1$, σ_{out}^2 is found only for the filters operated at stage I; $C_1, C_3(j^k)$, C_6 and $C_2(j^k)$. (Refer to Fig. 4.9a).

For C_1 ($\alpha=1$)

$h_{C_1}(i) = 1 \quad \forall i$, using (2.28) and the facts that $R_n(k)$ is symmetric, $R_{n_I n_R}(k)$ is antisymmetric and $R_n(k) = 0$ for k even it follows that:

$$\sigma_{out}^2, C_1 = \sum_{\ell=0}^{N-1} \sum_{i=0}^{N-1} R_n(\ell-i) =$$

$$\sigma_{out}^2, C_1 = NR_n(0) + 2 \sum_{\substack{i=1 \\ i \text{ odd}}}^{N-1} R_n(i) (N-i) \quad (2.30)$$

For $C_2(j^k)$: $\alpha=j$

$h_{C_2}(i) = (-1)^i$ using (5.28) it follows that:

$$\begin{aligned} \sigma_{out}^2, C_2(j^k) &= \sum_{\ell=0}^{N-1} \sum_{i=0}^{N-1} (-1)^i (-1)^\ell (j)^{N-1-i} (-j)^{N-1-\ell} |R_n(\ell-i) + \\ &+ jR_{n_I n_R}(\ell-i)| = \sum_{i=0}^{N-1} \sum_{\ell=0}^{N-1} (-j)^{\ell-i} [R_n(\ell-i) + R_{n_I n_R}(\ell-i)] \quad (5.31) \end{aligned}$$

$$\sigma_{out}^2, C_2 = \sum_{p=-(N-1)}^{N-1} [(-j)^p [R_n(p) + jR_{n_I n_R}(p)] [N-|p|]] \quad (2.32)$$

From (5.20) and (5.21) it follows that $R_n(k) = (-1)^{\lfloor \frac{k}{2} \rfloor} R_{n_I n_R}(k)$ for k odd. Using this fact and some more manipulations on (2.31) one obtains that:

$$\sigma_{out}^2, C_1 = \sigma_{out}^2, C_2(j^k) \quad (5.33)$$

(5.32) was also confirmed by a computer program for $N=6$ to 12.

For $C_6: \alpha=1$

$$h_{C_6}(i) = \{1, 1, 0, -1, -1, 1, 1, 0, -1, -1, \dots\}$$

Using (5.28) it follows that:

$$\sigma_{out}^2, C_6 = \sum_{i=0}^{N-1} \sum_{\ell=0}^{N-1} h_i h_\ell [R_n(\ell-i) + j R_{n_I n_R}(\ell-i)] \quad (5.34)$$

(5.34) was computed by a computer program for $N = 6$ to 12.

For $C_3(j^k), \alpha=j$

$$h_{C_3}(i) = \{1, -1, 0, 1, -1, 0, \dots\}$$

from (2.28) it follows that:

$$\sigma_{out}^2, C_3(j^k) = \sum_{i=0}^{N-1} \sum_{\ell=0}^{N-1} h_i h_\ell j^{N-i-1} (-j)^{N-1-\ell} [R_n(\ell-i) + j R_{n_I n_R}(\ell-i)]$$

(5.35)

(5.35) was found by a computer program for $N=6$ to 12. It turned out that for $N=6$ to 11 $\sigma_{out}^2; \hat{C}_6 = \sigma_{out}^2; \hat{C}_3(j^k)$.

Table 5.3 gives $\sigma_{out}^2/\sigma_{in}^2$ for the four filters operated at stage 1 for $N=6$ to 12. The results were obtained by a computer program using (5.30), (5.31), (5.34), and (5.35).

F \ N	6	7	8	9	10	11	12
C_1	11.34759	13.45106	15.3726	17.29422	19.3577	21.4202	23.3674
$C_3(j^k)$	7.39531	9.07436	11.5901	11.59012	13.1277	15.502	15.502
C_6	7.39530	9.07435	11.5901	11.59012	13.1277	15.502	15.502
$C_2(j^k)$	11.34758	13.45105	15.3726	17.29119	19.3572	21.4202	23.367

Table 5.3: $\sigma_{out}^2/\sigma_{in}^2$ for the filters operated at stage I.

טבלה 5.3: $\sigma_{out}^2/\sigma_{in}^2$ עבור המסננים המופעלים בשלב I.

For stages II and III using (5.28) one obtains Table 5.4. From (5.29) follows that $\sigma_{out}^2; \hat{C} = \sigma_{out}^2; \hat{C}(j^k)$:

F \ N	6	7	8	9	10	11
C_1	6	7	8	9	10	11
C_2	6	7	8	9	10	11
C_3	4	5	6	6	7	7
C_6	4	5	6	6	7	7

Table 5.4: $\sigma_{out}^2/\sigma_{in}^2$ for the filters operated at stage II and III ($\sigma_{out}^2, C = \sigma_{out}^2, C(j^k)$).

טבלה 5.4: $\sigma_{out}^2/\sigma_{in}^2$ עבור המסננים המופעלים בשלבים II ו-III. ($\sigma_{out}^2, C = \sigma_{out}^2, C(j^k)$)

Next the statistics of $\sqrt{z_R^2(N-1) + z_I^2(N-1)}$ is found when a tone is present.

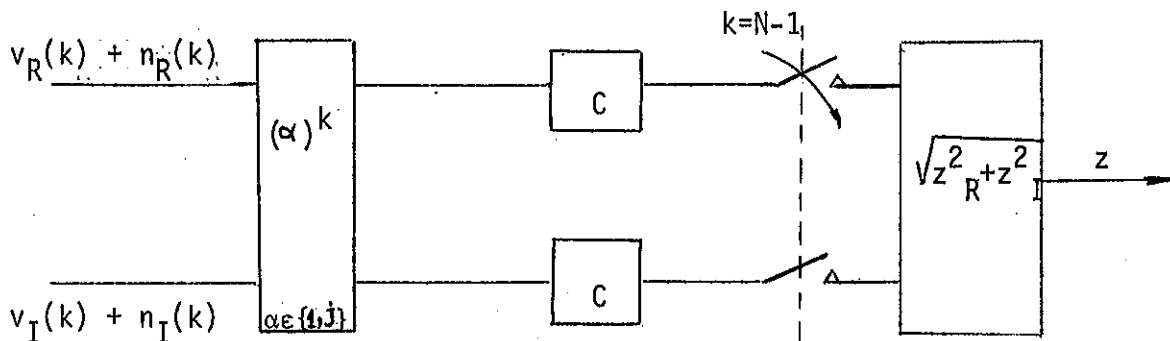


Fig. 5.6: The final processing unit.

ציור 5.6: יחידת העיבוד הסופית.

$$v_R(k) = A \cos\left(\frac{2\pi f}{f_{c_i}} k + \phi_1\right) \quad (5.36a)$$

$$v_I(k) = A \sin \left(\frac{2\pi f}{f_{C_i}} k + \phi_1 \right) \quad (5.36b)$$

define $\underline{v}(k)$ by:

$$\underline{v}(k) \triangleq v_R(k) + jv_I(k) \quad (5.37)$$

Define $u_R(k)$ and $u_I(k)$ by:

$$u_R(k) \triangleq v_R(k) + n_R(k) \quad (5.38)$$

$$u_I(k) = v_I(k) + n_I(k) \quad (5.39)$$

Also define $\underline{u}(k)$ by:

$$\underline{u}(k) = \underline{v}(k) + \underline{n}(k) \quad (5.40)$$

$\underline{n}(k)$ was defined by (5.22).

Referring to 5.3.2 it follows that:

$$u_R(k) \sim N[v_R(k), \sigma_{v_R}^2] \quad (5.41)$$

$$u_I(k) \sim N[v_I(k), \sigma_{v_I}^2] \quad (5.42)$$

$\sim N$ means Normally distributed. $\sigma_{v_i}^2$ is the power of the noise at each input (real, imaginary).

The filters are operated at stage s for N samples, hence:

$$z_R(N-1) = \sum_{\ell=0}^{N-1} h_{\ell} \operatorname{Re} \{ \alpha^{N-1-\ell} \underline{u}(N-1-\ell) \} \quad (5.43a)$$

$$z_I(N-1) = \sum_{\ell=0}^{N-1} h_{\ell} \operatorname{Im}\{\alpha^{N-1-\ell} \underline{u}(N-1-\ell)\} \quad (5.43b)$$

from (5.43) it follows that $z_R(N-1)$ and $z_I(N-1)$ are linear combinations of Gaussian variables, it follows that $z_R(N-1)$ and $z_I(N-1)$ are Gaussian:

$$\underline{z}(N-1) = \sum_{\ell=0}^{N-1} h_{\ell} \alpha^{N-1-\ell} \underline{u}(N-1-\ell) \quad (5.44)$$

Define z by:

$$z = |\underline{z}(N-1)| = \sqrt{z_R^2(N-1) + z_I^2(N-1)}$$

define x_R and x_I by:

$$x_R(N-1) = \sum_{\ell=0}^{N-1} h_{\ell} \operatorname{Re}\{\alpha^{N-1-\ell} \underline{v}(N-1-\ell)\} \quad (5.45a)$$

$$x_I(N-1) = \sum_{\ell=0}^{N-1} h_{\ell} \operatorname{Im}\{\alpha^{N-1-\ell} \underline{v}(N-1-\ell)\} \quad (5.45b)$$

define x by:

$$x = |\underline{x}(N-1)| = \sqrt{x_R^2(N-1) + x_I^2(N-1)} \quad (5.46)$$

then:

$$z_R(N-1) \sim N[x_R(N-1), \sigma_{\text{out}}^2] \quad (5.47a)$$

$$z_I(N-1) \sim N [x_I(N-1), \sigma_{out}^2] \quad (5.47b)$$

where σ_{out}^2 is given in tables 5.3 and 5.4.

Since $z_R(N-1)$ and $z_I(N-1)$ are statistically independent, it follows that z is Rician distributed (13, 14).

By (13) the distribution of z is given by:

$$f(z) = \frac{z}{2\pi\sigma_{out}^2} e^{-(z^2+x^2)/2\sigma_{out}^2} I_0\left(\frac{zx}{\sigma_{out}^2}\right) \quad (5.48)$$

where x is given by (5.46).

$I_0(x)$ is the modified Bessel function of order zero, given by:

$$I_0(x) = \frac{1}{2\pi} \int_0^{2\pi} e^{x \cos \theta} d\theta = \sum_{n=0}^{\infty} \frac{x^{2n}}{2^n (n!)^2} \quad (5.49)$$

The Raileigh distribution is a special case of the above with $x=0$ ($I_0(0) = 1$), i.e. no signal present:

$$f(z) = \frac{z}{2\pi\sigma_{out}^2} e^{-\frac{z^2}{2\sigma_{out}^2}} \mu(z) \quad (5.50)$$

$\mu(z)$ is the step function.

The Raileigh distribution has the following properties:

$$E\{z\} = \sigma_{out} \sqrt{\pi/2}; \quad E\{z^2\} = 2\sigma_{out}^2, \quad \sigma_z^2 = (2-\frac{\pi}{2}) \sigma_{out}^2 \quad (5.51)$$

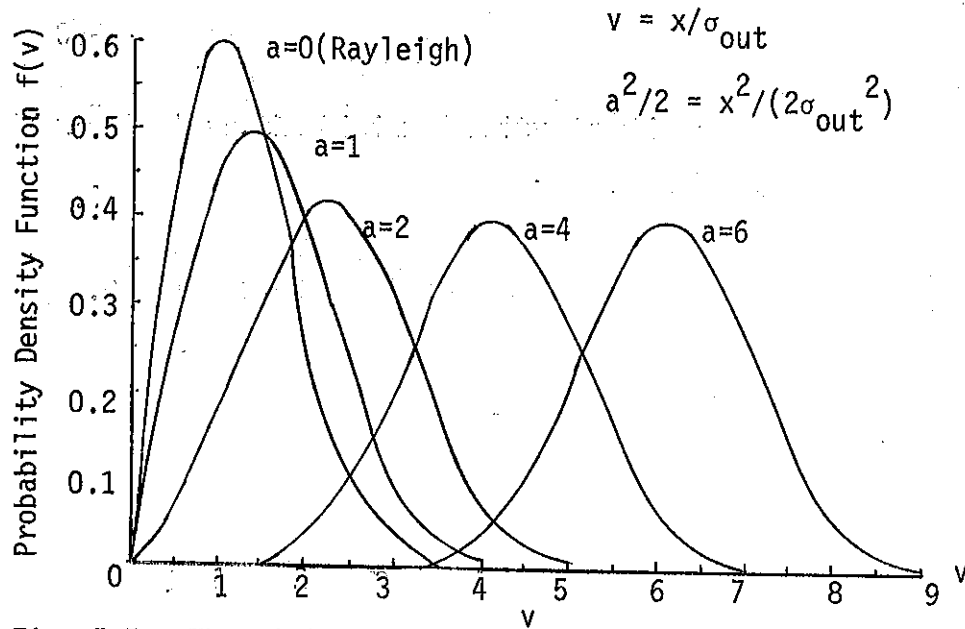


Fig. 5.7: The Rician density function.

ציור 5.7: פונקציית צפיפות מפורגת לפי רייס.

For $\frac{x^2}{2\sigma_{out}^2} \gg 1$ ($>10\text{db}$) the Rician distribution can be approximated by the Gaussian distribution.

5.4 Error Analysis at Stage s

At each stage four pairs of filters are operated. The filters output z is considered over an interval θ_s of length $\pi/2$. In each stage the question is in which of the four pairs of filters is the tone present.

5.4.1 Error Analysis at Stage I

Fig. 5.8 gives the plot of the four pairs of filters at stage I.

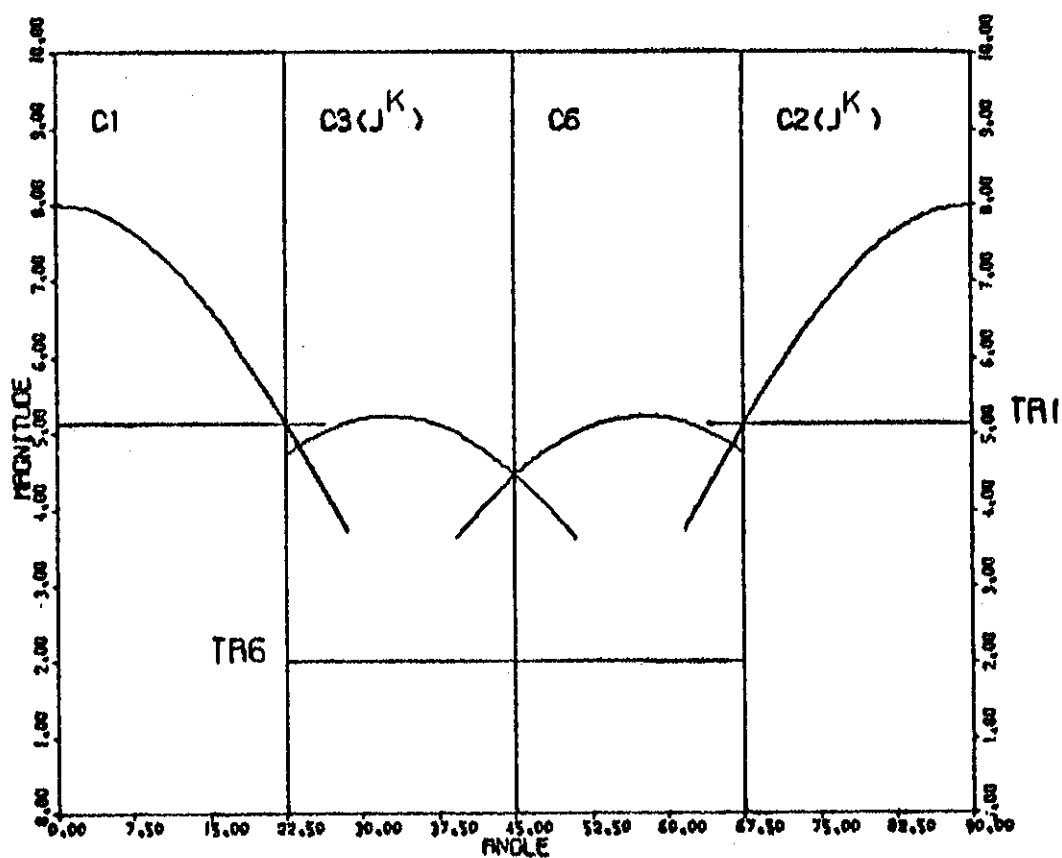


FIG. 5-8 : THE FOUR PAIRS OF FILTERS AT STAGE I
 ציור 5-8 : הצגה של הפילטרים בשלב I

θ_1 is assumed uniformly distributed, i.e.:

$$\theta_1 \sim U[0, \frac{\pi}{2}] \quad (5.52)$$

There are two kinds of errors:

- a. Errors associated with C_1 in the interval $0 < \theta_1 < \pi/4$
 - a.1 The output of the pair of C_1 's should have passed TR1 in the interval $0 < \theta_1 < \pi/8$ and did not pass it, because of the noise.
 - a.2 The output of the pair of C_1 's was expected not to pass TR1 in the interval $\pi/8 \leq \theta_1 < \pi/4$ and passed it because of the noise.
- b. Errors associated with $C_6, C_3(j^k)$ in the interval $\pi/8 < \theta_1 < 3\pi/8$.
 - b.1 The output of $C_6: z_{C_6}$ had to be bigger than the output of $C_3(j^k): z_{C_3(j^k)}$ in the interval $\pi/8 < \theta_1 < \pi/4$, but because of the noise the contrary happened.
 - b.2 z_{C_6} had to be smaller than $z_{C_3(j^k)}$ in the interval $\pi/4 < \theta_1 < 3\pi/8$. but because of the noise the contrary happened.
- c. Errors associated with $C_2(j^k)$ in the interval $\pi/4 < \theta_1 < \pi/2$.
 - c.1 The output of $C_2(j^k): z_{C_2(j^k)}$ was expected not to pass TR1 in the interval $\pi/4 < \theta_1 < 3\pi/8$ and passed it because of the noise.
 - c.2 $z_{C_2(j^k)}$ should have passed TR1 in the interval $3\pi/8 < \theta_1 < \pi/2$ but did not pass it because of the noise.

Another point has to be mentioned, if an error of any of the types a to c occurs in a neighbourhood of the points $\{\frac{\pi}{8}, \frac{\pi}{4}, \frac{3\pi}{8}, \frac{\pi}{2}\}$ of

bandwidth $\frac{\pi/2}{64}(\beta+1/2)$ where $1/2 < \beta < 1$:

The error will be corrected by the filters at the last stage and the frequency found will be within the permitted resolution. The permitted resolution is taken to be $\frac{\pi/2}{64}\beta$.

Calculating the Probability of Detection Error for C_1 and $C_2(j^k)$

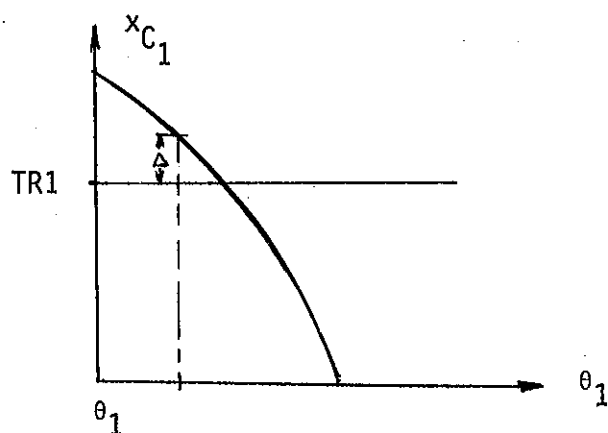


Fig. 5.9: The amplitude of the output of the pair C_1 .

ציור 5.9: האמפליטודה של יציאת זוג המסננים C_1 .

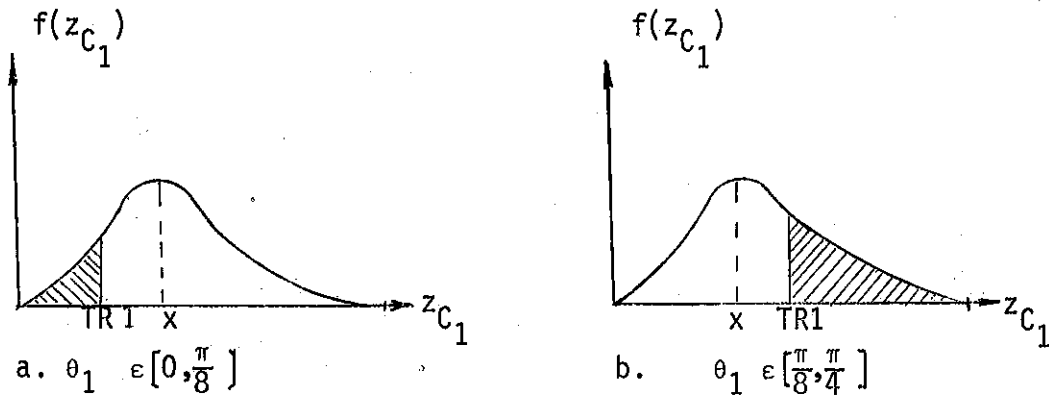
Let $Pe_1(\theta_1)|C_1$ be the probability of detection error at θ_1 (stage 1) constrained to C_1 .

define Δ and m by:

$$\Delta \triangleq |x - TR1| \quad (5.53)$$

$$m \triangleq \frac{\Delta}{\sigma_{out}} \quad (5.54)$$

The distribution of z_{C_1} is shown in Fig. 5.10.



ציור 5.10: הפילוג של z_{C_1} .

Fig. 5.10: The distribution of z_{C_1} .

In either (a) or (b) the probability of detection error is given by the shaded area.

$$Pe_1(\theta_1)|C_1 = \frac{1}{\sqrt{2\pi}} \int_m^{\infty} e^{-x^2/2} dx \quad (5.55)$$

(5.55) can be expressed more compactly by:

$$Pe_1(\theta_1)|C_1 = \frac{1}{2} \operatorname{erfc}(m/\sqrt{2}) \quad (5.56)$$

For $C_2(j^k)$ one obtains the same results as for C_1 since $\sigma_{out, C_1}^2 = \sigma_{out, C_2(j^k)}^2$.

Calculating the probability of detection error for C_6 and $C_3(j^k)$ in the interval $\pi/8 < \theta_1 \leq \pi/4$:

$z_{C_6}(\theta_1)$ is compared with $z_{C_3(j^k)}(\theta_1)$.

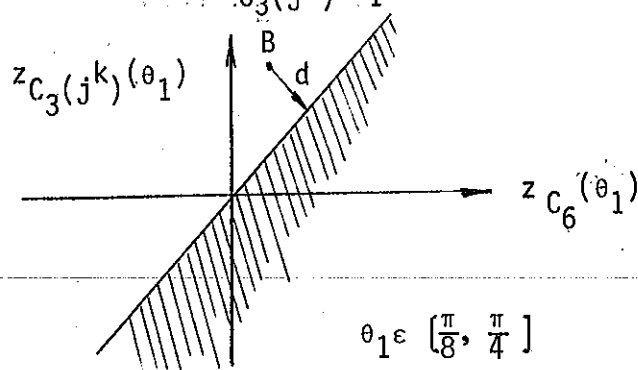


Fig. 5.11: Graphical presentation of the comparison of z_{C_6} and $z_{C_3(j^k)}$.

ציור 5.11: ייצוג גרפי של ההשוואה בין z_{C_6} ו- $z_{C_3(j^k)}$.

Referring to Fig. 5.11 the point B corresponds to $[x_{C_6}(\theta_1), x_{C_3(j^k)}(\theta_1)]$, i.e. no noise is present. An error occurs if $[z_{C_6}(\theta_1), z_{C_3(j^k)}(\theta_1)]$ is in the shaded area.

Assuming that z_{C_6} and $z_{C_3(j^k)}$ are statistically independent. This assumption is based on the fact that z_{C_6} and $z_{C_3(j^k)}$ cover different frequency bands.

A detection error occurs if:

$$z_{C_6}(\theta_1) < z_{C_3(j^k)}(\theta_1), \theta_1 \in [\frac{\pi}{8}, \frac{\pi}{4}]$$

$$d = \frac{z_{C_6}(\theta_1) - z_{C_3(j^k)}(\theta_1)}{\sqrt{2}} \quad (5.57)$$

define m by:

$$m = \frac{d}{\sigma_{out}} \quad (5.58)$$

hence:

$$\begin{aligned} Pe_1(\theta_1) | C_6, C_3(j^k) &= \frac{1}{\sqrt{2\pi}} \int_m^{\infty} e^{(-x^2/2)} dx = \\ &= \frac{1}{2} \operatorname{erfc} (m/\sqrt{2}) \end{aligned} \quad (5.59)$$

Now the average probability of detection error at stage I, Pe_1 can be computed.